

Design and Similitude Study of Composite Sandwich Beam

by

© Aninda Suvra Mondal

A thesis submitted to the
School of Graduate Studies
in partial fulfilment of the
requirements for the degree of
Master of Engineering

Faculty of Engineering & Applied Science
Memorial University of Newfoundland

October 2016

St. John's

Newfoundland

To my Family

Abstract

In this study, failure mode maps of composite sandwich panels are examined. Using Euler-Bernoulli beam theory, theoretical models are developed. The developed models are validated with established models in the literature. The models are compared with the established models using experimental data from literature. By comparing the developed models with the established models, it is concluded that the described models provide sufficient accurate results. Failure mode maps are constructed by using the non-dimensional form of the developed models. This concept of failure mode map is extended to provide a useful design tool for composite sandwich beam manufacturers. Also in this study, scaling laws are derived for a composite sandwich beam using the rules of similitude. Scaling laws define the relationships between a small specimen and a larger prototype structure. By using these scaling laws, it is possible to design a small scale model and by extrapolating the data from the small scale model, the behavior of a large scale prototype can be predicted. In the current study, similitude conditions for composite sandwich beams are developed for three loading conditions, uniformly distributed load, shear load and moment. To test the scaling laws a three-point bending test and a four-point bending test are taken from literature . Finite element analysis is used to obtain the stress distributions through the thickness of these composite sandwich models. Using the similitude conditions larger prototype of these models are created. Through-the-thickness stresses between the model and the prototype are compared and found to be in excellent agreement.

Acknowledgements

I wish to express my sincere thanks to my supervisor Dr. Sam Nakhla for his encouragement, guidance and constructive discussions during the development of this thesis.

I deeply appreciate the financial support of Research and Development Corporation of Newfoundland and Labrador (RDCNL) and the Graduate Fellowship from Memorial University. Without their support, this work could not have been possible.

Many thanks are extended to my colleagues for the useful discussions and suggestions throughout my work.

Finally, I would like to give my special thanks to my family. I am profoundly grateful for their love, support and understanding.

Contents

Abstract	i
Acknowledgements	ii
List of Abbreviations and Symbols	ix
1 Introduction	1
1.1 Composite Sandwich beams	2
1.2 Thesis Outline	4
2 Literature Review	6
2.1 Three-Point Bend Test	7
2.2 Four-Point Bend Test	8
2.3 Buckling of Sandwich beams	9
2.4 Finite Element Analysis	11
2.5 Similitude Study of Composites	12
3 Simplified Failure Mode Maps for the Design of Sandwich Beams	14
3.1 Introduction	16

3.2	Analysis	18
3.2.1	Normal Stress in the Facesheet	19
3.2.2	Shear Stress in the Core	21
3.2.3	Facesheet Debonding	23
3.2.3.1	Global Buckling	24
3.2.3.2	Wrinkling (Local Buckling)	25
3.3	Failure Mode Maps	29
3.4	Discussion and Conclusion	35
4	Structural Similitude for Sandwich Beam with Laminated Facesheet	36
4.1	Introduction	38
4.2	Mathametical Formulation	40
4.3	Numerical Analysis and Comparison with Experiments	48
4.3.1	Sandwich beam under uniformly distributed load	48
4.3.2	Comparison with three-point bending test	51
4.3.3	Comparison with four-point bending test	53
4.4	Discussion and Conclusion	55
5	Conclusion	57
5.1	Review	57
5.2	Future Work	60
	Bibliography	61
	Appendices	68

A	Non-dimensionalisation of Analytical Expressions	68
A.1	Normal Stress	68
A.2	Shear Stress	70
A.3	Global Buckling	71
A.4	Local Buckling (Wrinkling)	71

List of Tables

3.1	Geometric and material properties of sandwich beam constituents . . .	20
3.2	Comparison of predicted critical wrinkling load	29
4.1	Material properties of sandwich beam in distributed loading	49
4.2	Material properties of sandwich beam used in 3-point bending test . . .	52
4.3	Material properties of sandwich beam used in 4-point bending test . . .	54

List of Figures

1.1	Sandwich beam	2
3.1	Simply supported sandwich beam under uniform bending and moment	19
3.2	Cross section of a sandwich beam	19
3.3	Global buckling of the facesheet (facesheet debonding)	24
3.4	Idealised facesheet in global buckling	24
3.5	Local buckling of the top facesheet	26
3.6	Idealised facesheet in wrinkling	26
3.7	Failure mode maps for non-dimensional normal and shear stress . . .	31
3.8	Failure mode map for non-dimensional buckling and wrinkling	32
3.9	Contour plot for non-dimensional thickness of the facesheet (\bar{t}) and non-dimensional moduli (\bar{E})	33
3.10	Contour plot for non-dimensional mass, normal and shear stress . . .	34
4.1	Sandwich beam subjected to a distributed load, shear load and moment	40
4.2	Cross section of a sandwich beam	41
4.3	Cross-sectional geometry of a laminate sandwich beam	44

4.4	Normal stress distribution through the normalized thickness of model and prototype for distributed loading	50
4.5	Shear stress distribution through the normalized thickness of model and prototype for distributed loading	51
4.6	Shear stress distribution through the normalized thickness of model and prototype for shear loading	53
4.7	Normal stress distribution through the normalized thickness of model and prototype for applied moment	55

List of Abbreviations and Symbols

\mathbf{A}	Extensional stiffness matrix of the beam
AG_{eq}	Total shear rigidity of the beam
a	Unknown displacement parameter
b	Width of the beam
\bar{b}	Non-dimensional width of the facesheet
c	Thickness of the core
\bar{c}	Non-dimensional thickness of the core
\mathbf{D}	Bending stiffness matrix of sandwich beam
D_{11}	Bending stiffness of the sandwich beam
\bar{E}	Non-dimensional modulus of elasticity
E_c	Young's Modulus of the core
E_f	Young's Modulus of the facesheet
EI_{eq}	Total bending rigidity of the sandwich beam
G_c	Shear Modulus of the core
H_f	Bending rigidity of the facesheet
h_k	Height through the thickness
I_c	Second moment of area of the core at the midplane of the beam

I_f	Second moment of area of the facesheet at the midplane of the beam
I_{fo}	Second moment of area of the facesheet around its own axis
L	Length of the beam
\bar{L}	Non-dimensional length of the facesheet
L_w	Wrinkled length of the facesheet
λ_b	Scale factor of width
λ_D	Scale factor of bending stiffness
λ_M	Scale factor of moment
λ_q	Scale factor of distributed load
λ_V	Scale factor of shear force
λ_w	Scale factor of transverse deflection
λ_x	Scale factor of length
M	Applied Moment
\bar{M}	Non-dimensional moment
m_c	Mass of the core
m_f	Mass of the facesheet
m_s	Mass of the sandwich beam
n	Wave number
ν_c	Poisson's ratio of the core
P	Applied load
Π	Total potential energy
PMTPE	Principle of Minimum Total Potential Energy
P_{Allen}	Wrinkling load of Allen

P_b	Global buckling load of the facesheet
\bar{P}_b	Non-dimensional global buckling load
P_{Hoff}	Wrinkling load of Hoff and Mautner
$P_{Plantema}$	Wrinkling load of Plantema
$P_{Talreja}$	Wrinkling load of Talreja
P_w	Wrinkling load
\bar{P}_w	Non-dimensional wrinkling load
Q	First moment of area
\bar{Q}	Reduced stiffness matrix for a lamina
$q(x)$	Distributed load
ρ_c	Density of the core
ρ_f	Density of the facesheet
$\bar{\rho}$	Non-dimensional density
σ_f	Normal stress in the facesheet
t	Thickness of the facesheet
\bar{t}	Non-dimensional thickness of the facesheet
τ_c	Maximum shear stress in the core
$\bar{\tau}$	Non-dimensional shear stress
V	Maximum shear force applied
\bar{V}	Non-dimensional shear force
w	Displacement field of the beam
$w(x)$	Transverse deflection of the sandwich beam

Note: Other symbols not mentioned are defined in the text.

Chapter 1

Introduction

In high tech applications such as air-crafts, racing cars, spacecrafts, satellites, etc high performance designs of components are necessary. These structures need to be very light while having high stiffness and strength. Therefore, efficient and optimal structural design is required. Structural efficiency can be achieved by using efficient materials and by optimising the structural geometry. For an optimal design these factors need to be considered in the design process. Composites materials are very useful materials for the purpose of designing high performance structures. Composites have high stiffness and strength that can lead to a significant amount of weight reduction.

Composite materials consist of fibers embedded in a matrix. The physical and chemical properties of both fibers and matrix do not change. Yet the produced combined properties cannot be achieved by either of the constituents separately. Fibers are the principal load carriers while matrix keeps them together. Most commonly used fibers are glass, carbon, Kevlar etc. Polymers, metals, ceramics are used for

matrix materials.

The most common form of composites is called laminate. A laminate is made by stacking thin layers of fibers embedded in matrix. Fiber orientation and stacking sequence can be controlled to generate a wide range of mechanical and physical properties. Traditional materials such as aluminum, steel have equal properties irrespective of the direction. They are considered as isotropic materials. On the other hand the properties of composites strongly depends on the direction of the laminate.

1.1 Composite Sandwich beams

Sandwich beams are most commonly used in aeronautical applications though they are becoming popular day by day due to their widespread applications in both commercial, residential and offshore purposes. In recent years, sandwich beams have been used as building components in industrial, office and residential buildings particularly as roof and wall cladding due to their ability to improve the structural and thermal performance of buildings. Sandwich beams are a special class of composite materials with the features of low weight, high stiffness and high strength. They are fabricated by attaching two thin, strong, and stiff skins to a lightweight and relatively thick core as shown in Figure 1.1.

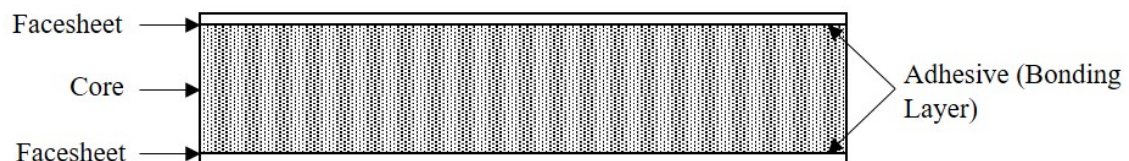


Figure 1.1: Sandwich beam

A sandwich beam is analogous to an I-beam in the sense that when subjected to bending, the flanges carry in-plane compression and tension loads and the web carries shear loads. In the case of sandwich beams the facesheets carry the in-plane compression and tension loads and the core carries the shear loads. As with a traditional I-beam, when the facesheets are further apart, the structure gains more stiffness. A thicker core can achieve the same stiffness and provides a low density, which results in a high stiffness-to-weight ratio. A typical sandwich panel consists of facesheets with a much thicker structural core in between. Materials such as steel, stainless steel, aluminum, composites are used as facesheet material. The function of the core is to support the facesheets so that they do not buckle and to keep them in relative position to each other. The core needs to be rigid in shear. The core of a sandwich structure can be of many material or architecture. In general, cores fall into four types (a) foam or solid core (b) honeycomb core (c) web core and (d) corrugated or truss core. Foam or solid cores can consist of balsa wood, foams, plastic materials with a wide variety of density and shear moduli. The facesheets are attached with the core with an adhesive. To keep the facesheets and the core cooperating with each other, the adhesive between the facesheets and the core must be able to transfer the shear forces between them. The adhesive must be able to carry shear and tensile stresses as well. The adhesive should be able to take up the same shear stress as the core. It is important that the facesheets properly adhere to the core to give the expected structural behavior.

The current study discusses the usage of sandwich beams for off-shore purposes. In spite of having these properties, the usage of composite sandwich beams are limited in offshore applications. A possible reason for this is that Scott and Sommella

[1] concluded that the acquisition cost per pound of composite material used can be increasingly greater than that of the equivalent steel component as its weight ratio diminishes. In other words composites are more expensive than conventional materials. Since 1971, there has been plenty of technological and manufacturing advancements of composites. Hence it may be questionable to rely on a report that has been written more than 40 years ago. Also, in their analysis no optimization tool was used for the composite. An unoptimized design can lead to a higher cost. The current study presents an optimization tool and similitude analysis of composite sandwich beams. The design of composite structures is more complicated than metal structures due to the fact that composites have orthotropic or anisotropic properties. However this non-isotropic behaviour of composites gives the designers an opportunity to tailor the properties to meet the design requirements. Although this improves the structural efficiency, it also increases the number of design parameters. Therefore, it is necessary to study how these parameters can be used to construct optimized and efficient sandwich beams.

1.2 Thesis Outline

This thesis consists of two manuscripts, They are submitted for publication.

- **Chapter 1** introduces the thesis and the research topic. It describes the objectives and provides a synopsis of the goals.
- **Chapter 2** provides a brief literature review on sandwich beams. The literature review is focused on foam core sandwich beams.

- **Chapter 3** is the first submitted manuscript that provides failure mode maps for four distinctive failure modes of sandwich beams for the purpose of providing a simple design tool for the designers and manufactures of sandwich beams. Analytical studies are conducted for global buckling, wrinkling, core shear and facesheet failures. A major contribution of the current work is introducing a new approach for predicting the wrinkling failure of sandwich beams. From the analytical expressions failure mode maps are constructed. The chapter explains how these failure mode maps can be used for designing an optimum sandwich beam.
- **Chapter 4** is the second manuscript, which consists of a study of similitude analysis of sandwich beams. Similitude studies can be found in the literature for sandwich beams with isotropic facesheets. This chapter presents similitude laws of sandwich beams with composite facesheets. The established similitude laws are applied in finite element analysis to verify the laws. The scaling laws provided in this chapter can be used to scale down a composite sandwich beam. By testing the scaled down model and by analysing the failure of the prototype can be predicted.
- **Chapter 5** reviews the research work and outcomes. Possible future work is also addressed.

Chapter 2

Literature Review

Due to their considerable structural importance, many publications dealing with sandwich beams are in existence. The aim of this chapter is to provide a brief review of sandwich beams that have been studied by researchers. The discussion and review is mainly focused only on sandwich beams with isotropic foam cores with thin metal or composite facesheets. A brief review of experimental and finite element studies made by previous researchers to investigate the buckling behavior of sandwich beams is also presented in this section. The review also discusses the various failure modes sandwich beams may experience. A brief review of similitude study on sandwich beams is also presented. Since before World War II, sandwich beams has been used in aircrafts and in many structural applications. The structural analysis of sandwich beams is being investigated since 1940s, especially in the aeronautical sector [2]. A simple guideline to the principal aspects of the theory of sandwich construction can be found in [2]. The behavior of sandwich structures of isotropic and composite materials is also discussed in [3]. For the past few decades, researchers have been studying

sandwich beams and many research papers have been published. These literature include analytical, experimental and finite element analysis of sandwich beams for various situations and loading conditions.

2.1 Three-Point Bend Test

In the past many researchers conducted various experimental studies of sandwich beams. These testing include three-point bend test, four-point bend test, compression test etc. Kim and Swanson [4] carried out experiments on foam core sandwich beams with carbon/epoxy facesheets under concentrated loading. The common failure modes observed by them were core failure in compression and shear, delamination and fiber failure in the facesheets. Their results showed that the failure modes and load levels can be predicted for sandwich structures under concentrated loading. Tagarielli et al. [5] experimented simply supported sandwich beams with glass-vinylester facesheets and PVC foam core in three-point bending test. They investigated the initial collapse modes, the mechanism that govern the post-yield deformation and parameters that set the ultimate strength of these beams. The failure modes of the sandwich beams in their experiments were face micro buckling, core shear and indentation. They presented analytical expressions for the finite deflection behavior of the beams which were in good agreement with the measured and finite element predictions. Kabir et al. [6] investigated sandwich beams with very thin aluminum face sheets under three-point bending loading conditions. The effect of the strength of the facesheets, thickness of the foam core and bending span length on the failure modes was studied. The experiments showed that thin facesheets sandwich beams experience indentation

failure under the loading roller. They constructed failure maps which can be used for the design of foam-cored sandwich beams with thin facesheets. Many researchers conducted the three-point bend test on metallic foam core sandwich beams. McCormack et al. [7] conducted three-point bend test on aluminum foam core sandwich beams. They estimated the initial failure load and the peak load for the failure modes. The dominant failure mode observed by them was core yielding while some of them failed due to face wrinkling. Yu et al. [8] investigated the response and failure of dynamically loaded sandwich beams with aluminum skin and aluminum foam core. The sandwich beams failed due to the cracking of the core in tension. In some tests the top facesheets failed due to wrinkling. Their final conclusion regarding the failure initiation was the failures occur due to local damage. Steeves and Fleck [9] demonstrated a systematic method for choosing the best materials for achieving minimum mass design of a sandwich beam under three-point loading conditions. They concluded that for low structural indices foam core is optimal, for higher structural load indices honeycomb core is optimal.

2.2 Four-Point Bend Test

Many researchers conducted four-point bend test on sandwich beams. Chen et al. [10] studied the behavior of sandwich composites in four point bending. The plastic collapse modes of sandwich beams have been investigated experimentally and theoretically for the case of an aluminum alloy foam with cold-worked aluminum face sheets. Plastic collapse is by three competing mechanisms: face yield, indentation and core shear. This study has shown that the analytical formulae given by limit

load analysis are in good agreement with the predictions. The formulae can be used directly in minimum weight design. Mohan et al. [11] performed four-point bend tests on alumina facesheets and alumina foam core with varying geometries to identify the failure modes. Analytical formulae for the failure modes were obtained and a failure mode map was constructed with non-dimensional parameters. Sokolinsky et al. [12] carried out four-point bend tests with aluminum facesheets and PVC foam core. The experimental results were compared with the classical sandwich theory, and with linear and geometrically nonlinear higher-order sandwich beam theory. Their work suggests the use of the linear higher-order theory instead of classical sandwich theory in design practice to better predict and avoid excessive bending deflections of sandwich beams under concentrated loading.

2.3 Buckling of Sandwich beams

One of the particular features of sandwich beam is the complicated buckling or instability behavior. Since buckling can quickly lead to failure this is of major concern to the designers. A typical sandwich beam may buckle in to distinctive ways, local buckling or wrinkling and global buckling. Many research papers have been published regarding the buckling behavior of sandwich beams. Roberts et al. [13] tested orthotropic FRP sandwich beams for buckling in uni-axial compression. They used two set of materials as the core material, balsa and PVC foam core. They measured the experimental elastic buckling load. They concluded that the buckling load for foam core beam is lower than the balsa core beam. Muc and Zuchara [14] studied a thin walled sandwich plate with laminated composite faces subjected to axial compression

loading for buckling. Stiftinger and Rammerstorfer [15] studied the local buckling of facesheets. Analytical and finite element analysis were carried out for compressive loading. Saoud and Grogneq [16] in their paper studied the theoretical elastic local/global buckling of rectangular sandwich plates under uniaxial or biaxial compression. In their formulation they presented the facesheets by Love-Kirchoff plate model and assumed that the core behaves as a 3D continuous medium. They solved the bifurcation equation for the problem for critical displacements and the associated buckling modes. They compared the results with finite element analysis which was in good agreement with the analytical solution. In an earlier study Douville and Grogneq [17] studied the local and global buckling of the facesheet in which they assumed the facesheet as Euler-Bernoulli beam and the core as 2D continuous solid. Léotoing et al. [18] presented applications of a novel unified model for sandwich beams with closed-form solutions for both global and local buckling. From their analytical study they obtained critical loads for a simply supported beam, through the calculation of two eigenvalues leading to the buckling modes. Jasion et al. [19] performed analytical, numerical and experimental studies of the the local and global buckling of facesheets in sandwich beams. They included the shear effect in their mathematical model. The derived governing equation was solved and the critical loads were compared with finite element analysis. Østergaard [20] studied the debonding of the facesheet due to local buckling. His study showed that the sensitivity to the face sheet imperfection results from interaction of local debond buckling and global buckling and the development of a damaged zone at the debond crack tip. From the literature review discussed above it can be asserted that researchers have conducted analytical, experimental and numerical methods to study and understand the behavior of sandwich beams

under various loading and boundary conditions. Researchers have conducted three-point and four-point bend tests, compression tests and various analytical methods to analyze the sandwich beam behavior. It can be noticed that the researchers did not use any design criteria for constructing the sandwich beams. The current study, focuses on developing a design tool for constructing optimized sandwich beams.

2.4 Finite Element Analysis

Finite element analysis is used by many researchers to compare with their experimental or analytical data. Mohan et al. [11] performed finite element analysis using ABAQUS finite element program. They simulated the brittle cracking of the facesheet for a four-point bend test. Wu et al. [21] in their paper modeled a sandwich beam as separated layers with appropriate constrains imposed between them. Their proposed FEM model was used to simulate the failure behavior of a FRP sandwich beam that is used in bus body. They compared the simulation results with other numerical predictions and the experiment. They concluded that their model is very efficient computationally for analyzing the failure issues of FRP sandwich structures. Pokharel and Mahendran [22] studied the inadequacy of conventional effective width formulae for sandwich beams with slender plates. They used experimental and finite element analysis to improve the design tool. Muc and Zuchara [14] studied a thin walled sandwich plate with laminated composite faces subjected to axial compression loading. They compared their analytical formulae with finite element analysis. The aim of their investigations was to point out the effects of the normal stresses and their influence on the sandwich behavior. Awad et al. [23] in their paper presented the

results of the experimental behavior and the non-linear finite element analysis (FEA) of the GFRP sandwich beam. The experimental works investigate the behavior of the GFRP sandwich beam, skincore interaction, and core behavior. A non-linear finite element model was developed to simulate the behavior of the skincore interaction, and the model was verified by comparing the results with those obtained from testing. Bambal [24] in his research developed a modeling approach to predict response of composite sandwich beams under static bending conditions. He attempted 2D and 3D solid with isotropic and orthotropic material properties in Finite Element (FE). He concluded that his proposed modeling proved to give reasonably accurate prediction for composite sandwich beams. From this brief review it can be seen that finite element analysis is a method vastly used by the researchers to simulate or compare their experiment or analytical results. In the current study, finite element analysis is used to observe the stress distributions through the thickness of sandwich beams.

2.5 Similitude Study of Composites

Similitude study is of great importance when it comes to testing of a structure. By using similitude laws a structure can be scaled down and experiments can be conducted on the scaled down structure. In many cases testing a full scale structure maybe impractical and expensive. For composite sandwich beams similitude rules are not straightforward as the number of parameters are many. Many researchers studied similitude analysis of composite beams. Similitude study of sandwich beams found in literature is done by Frostig and Simites [25, 26]. Their work presented scaling laws for sandwich beams with isotropic facesheets. In the current study similitude

conditions for sandwich beams with composite facesheets are developed.

Chapter 3

Simplified Failure Mode Maps for the Design of Sandwich Beams

A. S. Mondal, S. Nakhla

Faculty of Engineering and Applied Science
Memorial University of Newfoundland
St. John's, Newfoundland, Canada

An initial version of this work was published and presented in the *OCEANS '14 MTS/IEEE St. John's* conference. A version of this chapter is submitted in *Journal of Composites Part A: Applied Science and Manufacturing*. The author of this manuscript Aninda Mondal developed this work under the supervision of Dr. Sam Nakhla. Mr. Mondal's contribution to this paper is as follows:

- Performed all literature searches required for background information.
- Performed all the analysis and calculations.
- Analysed the results.
- Wrote the paper.

Dr. Sam Nakhla provided continuous technical guidance and editing of the manuscript. In this chapter, the manuscript is presented with altered figure numbers, table numbers and reference formats in order to match the thesis formatting guidelines set out by Memorial University.

Abstract: Failure modes of composite sandwich beams are outlined. Simplified theoretical predictions based on Euler-Bernoulli beam theory are introduced and discussed. Theoretical predictions are compared with other analytical models in open literature. Further comparisons are held with test data available in literature. These comparisons concluded sufficiently accurate predictions from simplified models. Finally, failure mode maps are constructed through consistent non-dimensionalization of geometric and material parameters extending the applicability of failure mode maps to provide useful design tool.

Keywords: Analytical Modelling, Sandwich Structure, Failure

3.1 Introduction

The use of sandwich beams mostly increased after World War II [2]. Since then, sandwich beams are becoming increasingly popular in sectors where high stiffness-to-weight ratio is necessary such as aerospace and marine industries. The work of Plantema [2] and Allen [27] focused on analysis of sandwich beams in terms of their stiffness and strength while further work in the literature [28–31] focused on their failure mechanisms. These failure mechanisms can be associated to either one of the sandwich beam components, i.e. facesheet or core. For example, Plantema [2] and Allen [27] presented discussions on sandwich beams buckling under in-plane loading. These discussions clarify the crucial aspects of buckling failure in which a facesheet debonds from the core. Facesheet debonding can occur in either one of two ways. Complete debonding of the face from core which is also known as global buckling. Alternatively a partial debonding may occur between face and core which is known as local buckling or facesheet wrinkling. Carlsson and Kardomateas [28], Nui and Talreja [29] and Mondal and Nakhla [30] studied buckling failure in various loading scenarios. Various analytical approaches were used in [28–30] to develop expressions for local buckling load conditions in sandwich beams. Daniel et al. [31] developed a detailed investigation of failure modes in sandwich composite beams and their associated prediction criteria. In their investigation they highlighted the dependency of failure modes on material properties and geometry of facesheets and core as well as loading conditions. They also stressed on the essential need to carefully conduct experiments on these beams to accurately delineate the conditions leading to failure. Also in [31] they outlined the failure modes in sandwich beams to be facesheet

failure, core failure, global buckling, wrinkling and indentation failure under concentrated load. Facesheet failure is explained to be due to uniaxial tensile or compressive stress, while the core commonly fails due to shear stresses [27]. Kim and Swanson [4], McCormack et al. [7], Kabir et al. [6] have shown in their experimental studies how the core of a sandwich beam fails in shear. Whereas facesheet debonding due to manufacturing defects or impact loading reduces beam stiffness and increases the potential of occurrence of global buckling [31]. Short wavelength buckling also known as facesheet wrinkling is mainly governed by the through-the-thickness direction core modulus. Finally, indentation failure takes place when external loads result in local yield of core associated with significant local deformation of the facesheet into the core. For example, a three-point bending test conducted without reinforcing the facesheet under the load application points. In order to enhance the understanding of failure modes in sandwich beams many researchers developed failure mode maps. Petras and Sutcliffe [32] constructed failure mode maps for facesheet failure, core shear, core crushing and wrinkling as a function of relative density and thickness of the facesheet. Shenhar et al. [33] and Steeves and Fleck [34] also presented failure mode maps for sandwich beams. Steeves and Fleck [34] constructed failure mode maps for microbuckling, wrinkling, core shear and indentation failure to deduce the aspect ratio of the facesheet and the core.

In the current study, simple analytical models are used to present an effective methodology to construct the failure maps of sandwich beams for the purpose of design optimization. Special attention is paid to the wrinkling failure mode to derive its analytical modes based on the classical approach of Winkler foundation. Analytical solutions for facesheet compressive failure, core shear failure, buckling and wrinkling

are presented. The solutions are compared for accuracy with real test data or other established solutions from literature. Failure maps are constructed for the failure modes. Contour plots of these failure modes are constructed as a function of non-dimensional core and facesheet thickness. From the contour plots, materials for the facesheet and core can be chosen and a non-dimensional core and facesheet thickness can be selected such that these failure modes can be avoided. To optimize the design, mass of the sandwich beam is also considered.

3.2 Analysis

This section aims at discussing simplified models to predict sandwich beam failure modes. For this purpose, a unified formulation based on Euler-Bernoulli beam (E-B beam) theory is used. Failure modes discussed in this section are facesheet failure, core failure, global buckling and wrinkling of facesheet. A general problem of a simply supported sandwich beam is used throughout the analysis. The beam is under distributed load $q(x)$ and distributed moment $m(x)$ as illustrated in Figure 3.1. The detailed geometry of the cross section is shown in Figure 3.2.

For the purpose of comparison with test data, numerical predictions developed within are compared to test results documented in [31]. Carbon/epoxy (AS4/3501-6) and PVC foam Divinycell H250 are generally used for facesheet and foam core unless otherwise mentioned. The material properties of these constituents and beam geometry are adopted from [31] and provided in Table 3.1.

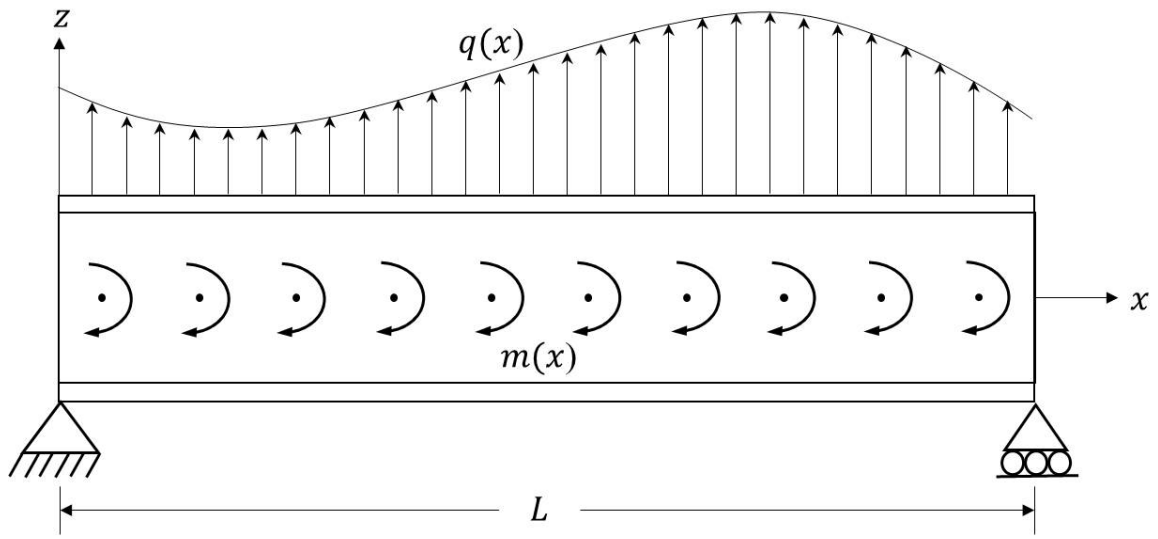


Figure 3.1: Simply supported sandwich beam under uniform bending and moment

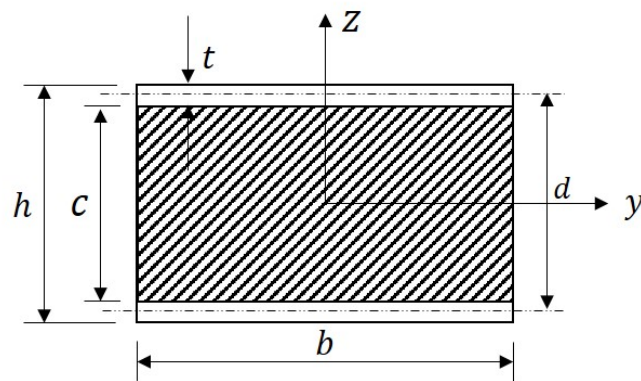


Figure 3.2: Cross section of a sandwich beam

3.2.1 Normal Stress in the Facesheet

As expressed by Daniel et al. [31] uniaxial stresses, tensile or compressive is responsible for facesheet failure. This is explained by realizing that the facesheet is responsible for carrying normal stresses due to its increased normal stiffness in comparison to the soft core material. In [31] they recorded their observation by testing a sandwich beam with carbon/epoxy face and aluminum honeycomb core. They ex-

Table 3.1: Geometric and material properties of sandwich beam constituents [31]

	Carbon/Epoxy	Foam H250
Density (kg/m^3)	$\rho_f = 1620$	$\rho_c = 250$
Young's Modulus (MPa)	$E_f = 147000$	$E_c = 403$
Shear Modulus (MPa)	-	$G_c = 117$
Poisson's Ratio	$\nu_f = 0.25$	$\nu_c = 0.32$
Compressive Strength (MPa)	$\sigma_{allow} = 1930$	-
Shaer Strength (MPa)	-	$\tau_{allow} = 5$
Thickness (mm)	$t = 0.8$	$c = 25.4$
Width (mm)	$b = 26$	
Length (mm)	$L = 406$	

plained the observed failure to be dominantly the result of compressive stresses in the face. Moreover, they concluded the adequacy of linear bending theory to predict facesheet failure. Consequently in this section the normal stress in the facesheet is predicted using Euler-Bernoulli beam theory for built-up sections as explained in Gere [35]

$$\sigma_f = \frac{E_f M z}{E_f I_f + E_c I_c} \quad (3.1)$$

where, M is the maximum moment at the cross-section, E_f and E_c are the homogenized moduli of the facesheet and core, respectively, and I_f , I_c are the second moment of area of the face and core, respectively obtained at the beam midplane. The homogenized modulus of the facesheet, E_f , can be obtained using the extensional stiffness matrix \mathbf{A} as demonstrated by Mallick [36]. The facesheet is assumed to be symmetric

around its own mid-plane to guarantee hygrothermal stability, hence

$$\mathbf{A} = \begin{bmatrix} A_{11} & A_{12} & 0 \\ A_{21} & A_{22} & 0 \\ 0 & 0 & A_{33} \end{bmatrix} \quad (3.2)$$

The homogenized modulus E_f can be expressed as

$$E_f = \frac{A_{11}A_{22} - A_{12}^2}{tA_{22}} \quad (3.3)$$

In a four-point bending test conducted by Daniel et al. [31] compressive failure of facesheet was observed. The sandwich beam had an aluminum honeycomb core which has a longitudinal modulus of 9.5 MPa. The documented compressive failure moment is 1.09 kN.m. The calculated predicted normal stress in the facesheet using Equation (3.1) is 2061 MPa where the compressive strength of carbon/epoxy facesheet is 1930 MPa. The percentage difference of prediction of compressive failure using Equation (3.1) is 6.8%. Therefore, the expression in Equation (3.1) provides sufficiently accurate prediction of the facesheet compressive failure.

3.2.2 Shear Stress in the Core

Contrary to normal stresses the core of a sandwich beam is responsible for carrying shear stresses [31]. Allen [27] modified the shear stress equation based on E-B homogenous beam theory to account for a beam of compound cross-section.

$$\tau = \frac{V}{EI_{eq}b} \Sigma QE \quad (3.4)$$

where, V is the maximum shear force, EI_{eq} is the total bending rigidity of the sandwich beam and the summation term is carried out over the product of the first moment of area, Q and the corresponding modulus E of the section constituents. Allen [27] also explained that the shear stress is maximum at the mid-plane of the sandwich beam, if symmetric. Therefore, Equation (3.4) can be evaluated at the mid-plane as

$$\tau_c = \frac{V}{EI_{eq}} \left(\frac{E_f t d}{2} + \frac{E_c c^2}{8} \right) \quad (3.5)$$

where, t is the thickness of the facesheet, c is the thickness of the core and

$$EI_{eq} = E_f I_f + E_c I_c \quad (3.6)$$

Daniel et al. [31] documented that shear failure occurs in the vicinity of the proportional limit of the shear stress-strain curve of the core. Therefore, shear stress failure can be predicted using Equation (3.5). As Equation (3.5) is developed using E-B beam theory, it may over-predict the value of the shear stress. Other researchers developed further solutions to increase the accuracy of shear stress prediction in the core. For example, Steeves and Fleck [34] elected to use the nonlinear solution developed by Chiras et al. [37] to predict the shear stress in a sandwich beam. This nonlinear solution is based on Timoshenko beam theory for the case of rigid-ideally plastic core and elastic facesheets. The expression developed by Chiras et al. [37] is

$$\tau_c = \frac{2V - 8E_f b(t/L)^3 \delta}{2bd} \quad (3.7)$$

where,

$$\delta = \frac{2VL^3}{48EI_{eq}} + \frac{2VL}{4AG_{eq}} \quad (3.8)$$

where, AG_{eq} is the total shear rigidity of the sandwich beam which can be approximated as the shear rigidity of the core material. A three point bending test was conducted by Daniel et al. [31]. The span length of the beam was 380 mm. They documented that non-uniform shear deformation starts close to the proportional limit of the stress-strain curve of the H250 foam which is 2.55 MPa. For this case, the predicted shear stress in the core using Equation (3.5) and (3.7) are 2.47 MPa and 2.42 MPa, respectively. The percentage differences of the calculated predicted load are negative 3% and 5.1%, respectively. Therefore, the linear theory (E-B beam theory) provides sufficiently accurate prediction to the onset of shear failure.

3.2.3 Facesheet Debonding

A sandwich beam is constructed by adhesively bonding two thin facesheets on both sides of a soft core material, hence there exists the possibility of facesheet debonding from core during load application. Facesheet debonding may occur due to fabrication imperfections in the sandwich beam or external impact loading. Debonding results in the reduction of facesheet bending stiffness. As stated earlier buckling of the facesheet can be global or local, alternatively referred to as global buckling and wrinkling, respectively. Many researchers have developed expressions to predict the buckling and wrinkling loads for a sandwich beam using various methods.

3.2.3.1 Global Buckling

Bauchau and Craig [38] provide an expression to predict global buckling load by idealizing the facesheet as a simply supported beam resting on an elastic foundation as shown in Figure 3.3 and 3.4. The stiffness of the elastic foundation is defined in terms of the transverse modulus of the core, E_c . For this purpose, they used the Principle of Minimum Total Potential Energy (PMTPE) based on E-B beam theory.

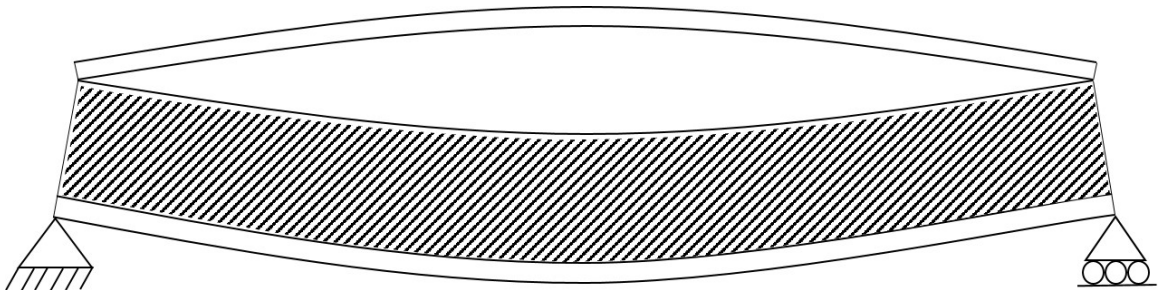


Figure 3.3: Global buckling of the facesheet (facesheet debonding)

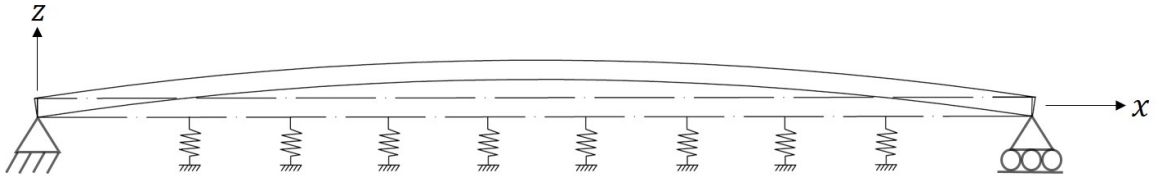


Figure 3.4: Idealised facesheet in global buckling

The global buckling load as developed by Bauchau and Craig [38] is expressed in terms of a wave number, n as

$$P_b = \frac{n^2 \pi^2 E_f b t^3}{12 L^2} + \frac{E_c L^2}{n^2 \pi^2} \quad (3.9)$$

They identified the minimum global buckling load to correspond to a wave number of unity. Meanwhile, in the tests conducted by Daniel et al. [31] no global buckling was observed in the absence of manufacturing imperfections and impact damage. Therefore, theoretical values of global buckling load is used in this study without comparisons with test data.

3.2.3.2 Wrinkling (Local Buckling)

In two four-point-bending tests conducted by Daniel et al. [31] wrinkling of the facesheet was observed for foam core sandwich beams. There exists in the literature a number of expressions to predict facesheet wrinkling load. Hoff and Mautner derived an expression as explained by Carlson and Kardamatas [28] using a linear decay function. Plantema [2], Allen [27], Nui and Talreja [29] also established expressions to predict the minimum wrinkling load. Recently, Mondal and Nakhla [30] developed an expression based on E-B beam theory using the classical approach of Winkler foundation. This approach is consistent with the one developed by Bauchau and Craig [38] for global buckling. Principle of Minimum Total Potential Energy is used to derive the expression. Face wrinkling is characterized by local instability or wrinkling as shown in Figure 3.5 which has shorter wavelength than those associated with global buckling of the plate. In order to develop a mathematical model for wrinkling both relative displacement and slope are assumed to be zero at the boundaries of the wrinkling length. Therefore, wrinkling of facesheet can be idealized as double cantilever (clamped-clamped) beam resting on elastic foundation as shown in Figure 3.6.

The wrinkled length L_w of the beam is considered for the analysis, where $L_w =$

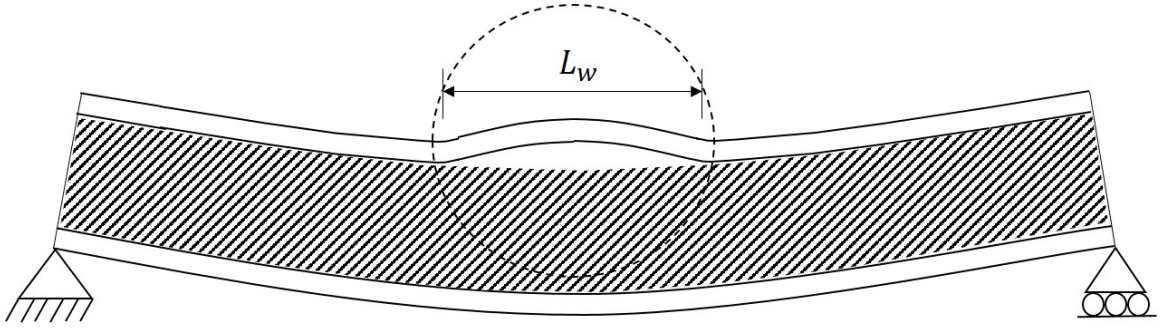


Figure 3.5: Local buckling of the top facesheet

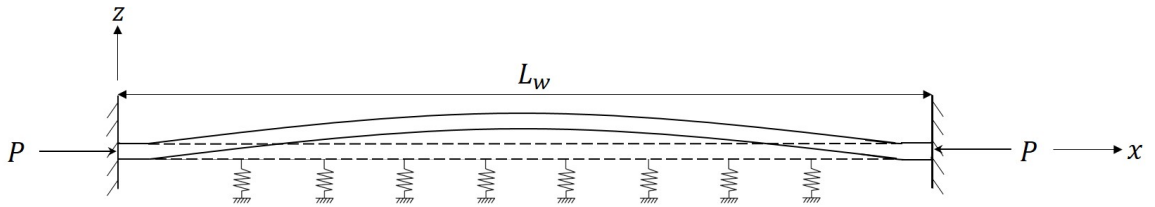


Figure 3.6: Idealised facesheet in wrinkling

αL ($0 < \alpha < 1$). The bending stiffness of the facesheet is

$$H_f = E_f I_{f_o} \quad (3.10)$$

where, I_{f_o} is the second moment of area of the face around its own centroid or mid-plane. The load required to cause the facesheet to wrinkle is predicted using PMTPE approach with the following assumed displacement field

$$w(x) = a(\xi^2 - 2\xi^3 + \xi^4) \quad (3.11)$$

where, $\xi = x/L$ and a is an unknown displacement parameter. Total potential energy of the system, Π , is the superposition of strain energies due to the bending of the face, strain energy in the elastic foundation (the core) and potential energy of the

applied load, P .

$$\Pi = \frac{1}{2} \int_0^{L_w} H_f \left(\frac{d^2 w}{dx^2} \right)^2 dx + \frac{1}{2} \int_0^{L_w} E_c w^2 dx - \frac{1}{2} \int_0^{L_w} P \left(\frac{dw}{dx} \right)^2 dx \quad (3.12)$$

Substituting Equation (3.11) into (3.12) and integrating we get,

$$\Pi = H_f \frac{2a^2}{5L_w^2} + \frac{E_c L_w a^2}{1260} - \frac{Pa^2}{105L_w} \quad (3.13)$$

The total potential energy is expressed here as a function of unknown amplitude a .

Applying the PMTPE theory,

$$\frac{d\Pi}{da} = \left(\frac{4H_f}{5L_w^3} + \frac{E_c L_w}{630} - \frac{2P}{105L_w} \right) a = 0 \quad (3.14)$$

Either a is zero or the term in parenthesis is zero. In the latter case, $P = P_w$ is the wrinkling load at which wrinkling of the facesheet occurs.

$$P_w = \frac{42H_f}{L_w^2} + \frac{E_c L_w^2}{12} \quad (3.15)$$

An expression for the wrinkling length can be derived by differentiating Equation (3.15) with respect to the length (L_w). The expression for the minimum value of wavelength L_w corresponds to minimum P_w is

$$L_w = \sqrt[4]{\frac{504H_f}{E_c}} \quad (3.16)$$

Equation (3.16) can be substituted into (3.15) to find the minimum wrinkling load

for the facesheet. The expressions derived by Hoff and Mautner which is explained by Carlson and Kardomateas [28], Plantema [2], Allen [27] and Nui and Talreja [29] are shown in Equations (3.17 - 3.20) respectively. Nui and Talreja [29] provided solutions for short wavelength and long wavelength wrinkling. From the experimental data in [31] and comparing them with the solutions provided by Nui and Talreja [29] it was seen that wrinkling of the facesheet in the test was a short wavelength wrinkling. Therefore, the solution for short wavelength provided by Nui and Talreja [29] is given in Equation (3.20).

$$P_{Hoff} = 0.91bt\sqrt[3]{E_f E_c G_c} \quad (3.17)$$

$$P_{Allen} = btB_1 E_f^{1/3} E_c^{2/3} \quad (3.18)$$

where, $B_1 = 3[12(3 - \nu_c)^2(1 + \nu_c)^2]^{-1/3}$

$$P_{Plantema} = 0.825bt\sqrt[3]{E_f E_c G_c} \quad (3.19)$$

$$P_{Talreja} = bt \left[\left\{ \frac{3E_c}{2(1 + \nu_c)(3 - \nu_c)} \right\}^{2/3} E_f^{1/3} + \frac{(1 - \nu_c)E_c}{(1 + \nu_c)(3 - \nu_c)} + \left\{ \frac{E_c}{(1 + \nu_c)(3 - \nu_c)} \right\}^{4/3} \left(\frac{3}{2E_f} \right)^{1/3} \right] \quad (3.20)$$

Daniel et al. [31] documented that facesheet wrinkling failure was observed for sandwich beams with foam cores. They reported that the wrinkling behavior is controlled by the core modulus. In a four-point bending test of a sandwich beam with Divinycell H100 foam core they measured a critical wrinkling load of 14 kN. From their test a comparison is held between analytical prediction and their measured wrinkling load. The results from this comparison is provided in Table 3.2. Comparing the predicted minimum wrinkling loads in Table 3.2 it can be seen that the current method provides

sufficiently accurate prediction of minimum wrinkling load.

Table 3.2: Comparison of predicted critical wrinkling load

	Wrinkling Load in kN (Percentage comparison with [31])
Current	17.8(%27.1)
Hoff and Mautner [28]	18.8(%34.3)
Allen [27]	16.6(%18.6)
Plantema [2]	17.0(%21.4)
Nui and Talreja [29]	17.2(%22.9)

3.3 Failure Mode Maps

In this section failure mode maps are constructed for different failure modes discussed in the previous section. Using E-B beam theory as the unified basis for constructing these maps guarantees consistent and straight forward approach. Also, consistent non-dimensional parameters are used while constructing these maps for the same purpose of unified basis. Moreover, the knowledge gain in comparing analytical predictions with test results from [31] is introduced into the developed maps. Finally, the constructed maps are discussed and proposed as a design tool for sandwich construction. Non-dimensional parameters are defined based on material properties and geometry of the sandwich beam constituents. Allowable values for facesheet normal and core shear stresses are used to obtain the non-dimensional failure modes of facesheet and core materials, respectively. While Euler buckling loads for simply supported and clamped-clamped beams are used for global buckling and wrinkling of the facesheet, respectively. Finally, the total thickness of the sandwich beam is used to ob-

tain non-dimensional dimensions of the cross-section. Therefore, the non-dimensional dimensions of the cross section and sandwich beam length can be expressed as

$$\bar{t} = \frac{t}{h}; \bar{c} = \frac{c}{h}; \bar{b} = \frac{b}{h}; \bar{L} = \frac{L}{h} \quad (3.21)$$

Non-dimensional normal stress in the facesheet is obtained from Equation (3.1)

$$\bar{\sigma} = \bar{M} \frac{3\bar{t}(\bar{c} + \bar{t})}{6\bar{t}(\bar{c} + \bar{t})^2 + \bar{E}\bar{c}^3} \quad (3.22)$$

where, $\bar{M} = M/\sigma_{allw}bt(d/2)$. From the test conducted in [31] it is found that $\bar{M} = 1.94$.

Non-dimensional shear stress in the core is obtained from Equation (3.5)

$$\bar{\tau} = \bar{V} \left[\frac{\bar{c}}{\bar{c} + \bar{t}} + \frac{\bar{E}}{4} \frac{\bar{c}^3}{\bar{t}(\bar{c} + \bar{t})^2} \right] \quad (3.23)$$

where, $\bar{V} = V/\tau_{allw}bc$. From the test conducted in [31] it is found that $\bar{V} = 1.03$. Non-dimensional global buckling load of the facesheet is obtained from Equation (3.9)

$$\bar{P}_b = 1 + \frac{12\bar{E}\bar{L}^4}{\pi^4\bar{b}\bar{t}^3} \quad (3.24)$$

Non-dimensional wrinkling load of the facesheet is obtained from Equation (3.15).

$$\bar{P}_w = 0.6161 \sqrt{\frac{\bar{E}\bar{L}^4}{\bar{b}\bar{t}^3}} \quad (3.25)$$

Using the properties of carbon/epoxy facesheet and H250 foam core given in Table 3.1 the following failure mode maps are constructed. Failure mode maps of non-dimensional normal and shear stress are constructed from Equation (3.22) and (3.23). To account for safety factor of 2, $\bar{M} = 1$ and $\bar{V} = 0.5$ are considered. The failure mode maps for normal and shear stresses are shown in Figure 3.7. In Figure 3.7

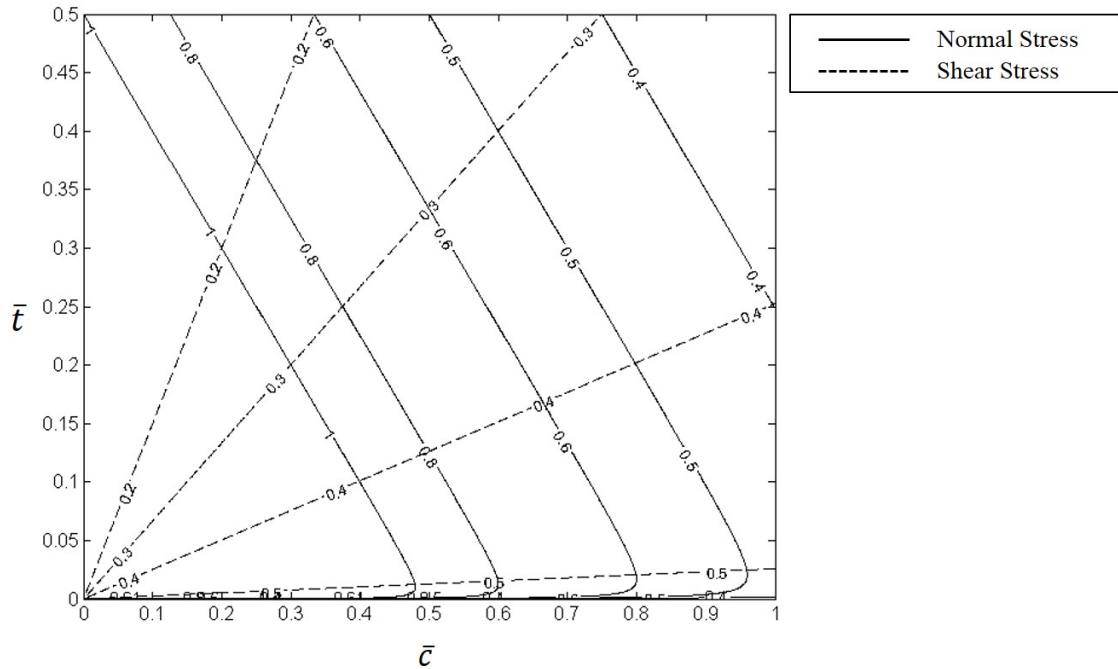


Figure 3.7: Failure mode maps for non-dimensional normal and shear stress

the values on the lines denotes the values of non-dimensional stresses. The solid line consisting a value of unity indicates that along this line the normal stress in the facesheet is equal to the allowable stress of the facesheet. For design purpose, the value of \bar{t} and \bar{c} should be such that the contour lines has a value less then unity as this indicates that the stresses will be less than their corresponding allowable stresses. Non-dimensional global buckling and wrinkling load are plotted in Figure 3.8. From

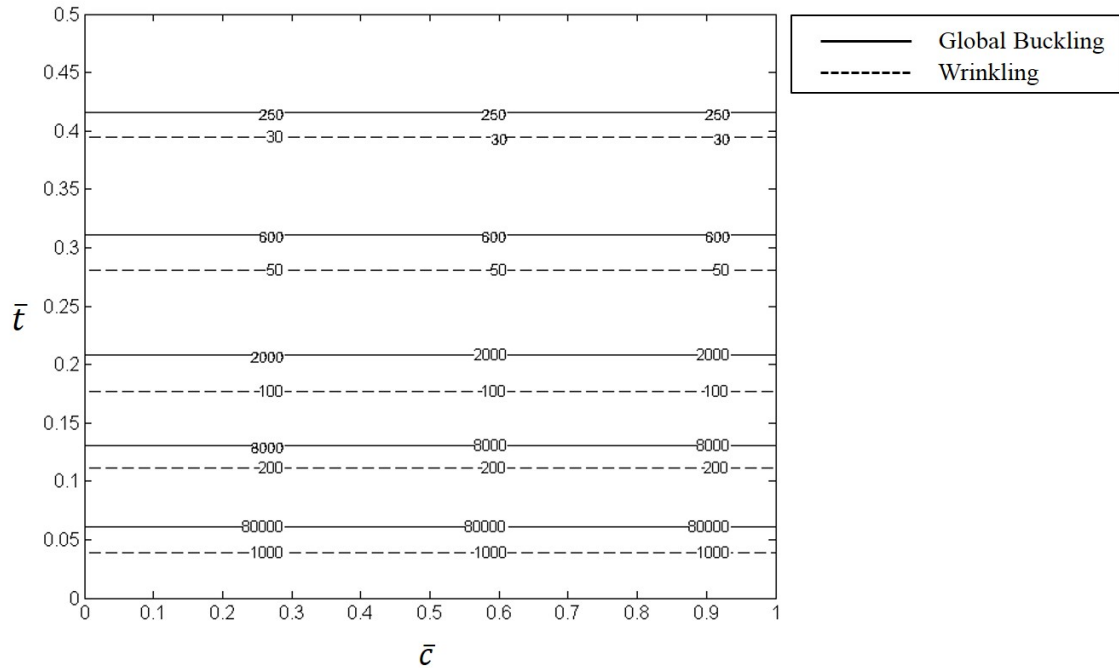


Figure 3.8: Failure mode map for non-dimensional buckling and wrinkling

Figure 3.8 it is noticeable that global buckling load is higher than wrinkling load. This indicates that wrinkling is likely to occur before buckling takes place. This is also verified by the experiments conducted by Daniel et al. [31] where wrinkling was observed while no debonding of the facesheet was observed for foam core sandwich beams. Therefore, wrinkling should be considered more critical than buckling while designing a sandwich beam. Figure 3.8 also indicates that the buckling and wrinkling phenomena are independent of core thickness. This enables us to plot \bar{P}_b and \bar{P}_w as a function of \bar{t} and \bar{E} . A semi-log plot is constructed for \bar{t} vs $1/\bar{E}$ in Figure 3.9. From a designers perspective let us say, we want to choose a suitable facesheet and core. A suitable ratio of E_f/E_c can be chosen from Figure 3.9. It is expected that the facesheet of the sandwich beam has high value of \bar{P}_w so that it does not fail at a

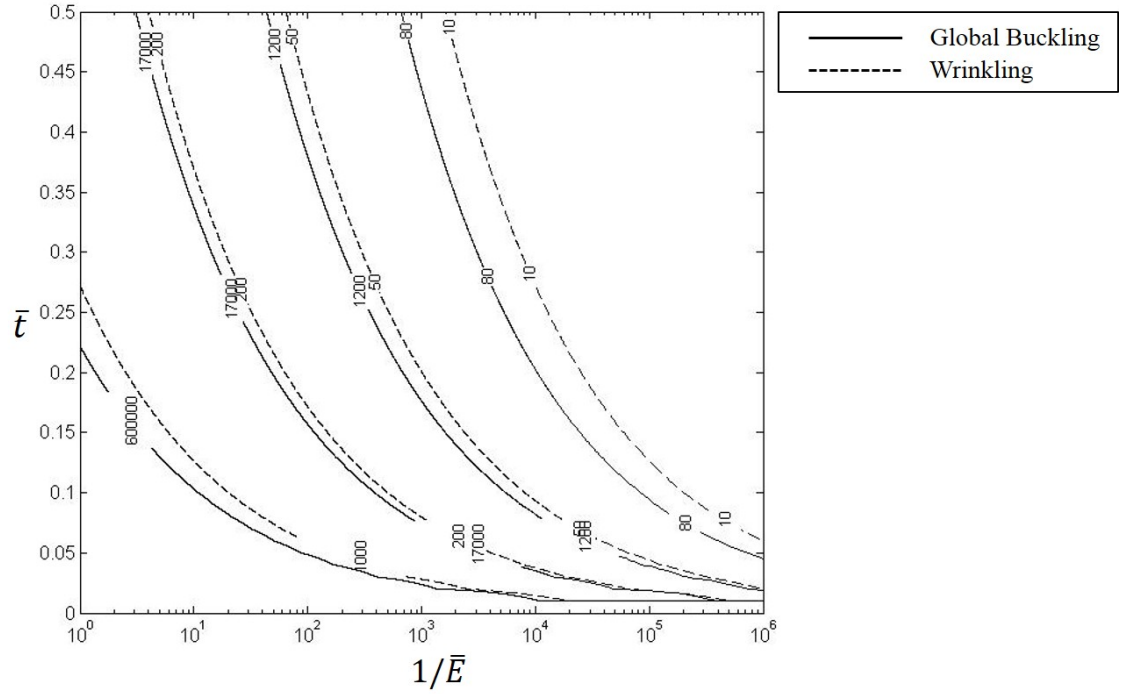


Figure 3.9: Contour plot for non-dimensional thickness of the facesheet (\bar{t}) and non-dimensional moduli (\bar{E})

low wrinkling load. Once the material is selected, the non-dimensional thickness (\bar{t}) of the facesheet can be selected using Figure 3.9. While choosing for a suitable (\bar{t}) it is necessary that the sandwich beam is optimized.

Sandwich beam can be optimized by minimising the mass of the beam. If the density of the facesheet and the core is ρ_f and ρ_c , respectively, then the mass (m_s) of a sandwich beam is the sum of the mass of the facesheets (m_f) and the core (m_c).

$$m_s = m_f + m_c \quad (3.26)$$

where, $m_f = 2bLt\rho_f$ and $m_c = bLc\rho_c$. Non-dimensional mass of the beam is obtained

from Equation (3.26).

$$\bar{m} = \frac{m_s}{bLh\rho_f} = (2\bar{t} + \bar{c}\bar{\rho}) \quad (3.27)$$

where, $\bar{\rho} = \rho_c/\rho_f$. Equation (3.27) is plotted in Figure 3.10 along with the non-dimensional normal and shear failure mode maps. Figure 3.10 shows that the thick-

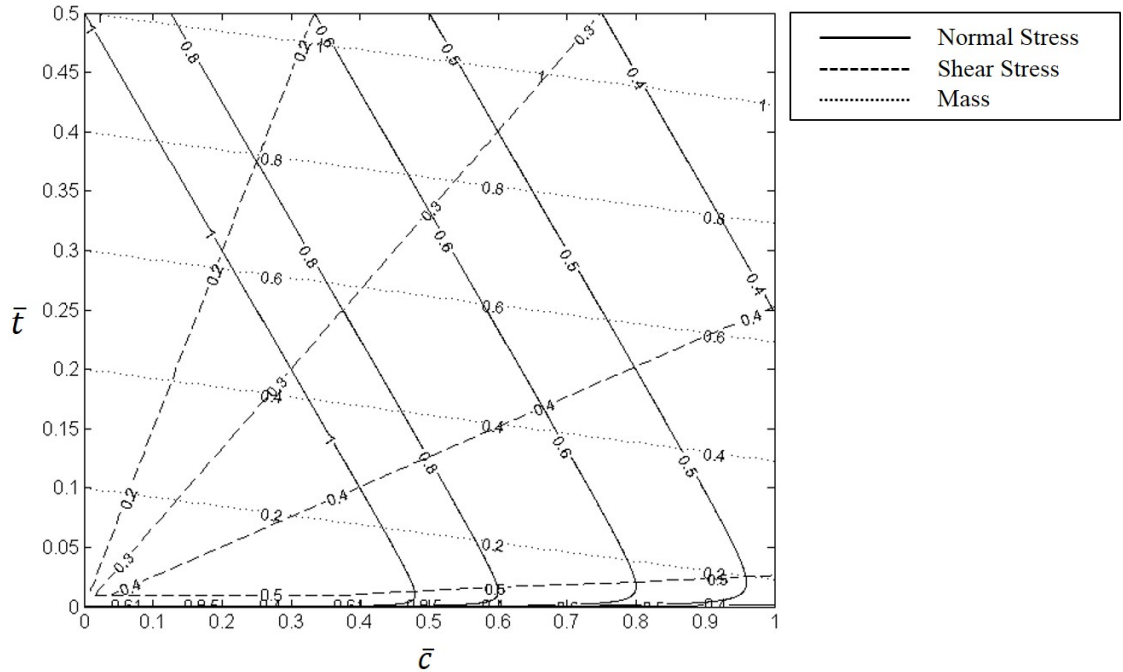


Figure 3.10: Contour plot for non-dimensional mass, normal and shear stress

ness of the facesheet has higher contribution over the mass of the sandwich beam than the thickness of the core. Figure 3.10 suggests that the thickness of the facesheet should be kept low for designing a lightweight sandwich beam. Once a suitable \bar{t} is chosen from Figure 3.9 and 3.10 a value of \bar{c} can also be selected. Then the selected values of \bar{t} and \bar{c} can be verified from Figure 3.10 whether it is in the failure region or not.

3.4 Discussion and Conclusion

A general discussion of failure modes of sandwich beams is presented for the purpose of arriving at unified basis. Euler-Bernoulli beam theory and the classical approach of Winkler foundation are used as the unified basis. A special attention is made to develop a simplified model for wrinkling failure. The developed model utilizes beam theory and Winkler foundation approach within the framework of the PMTPE. The developed wrinkling failure model is in good agreement with other analytical solutions published in literature. Additionally all analytical predictions of presented failure modes are compared to test data and other analytical solutions available in literature. Comparisons prove adequate predictions of all simplified failure models. Furthermore non-dimensional failure mode maps are presented for facesheet compressive failure, core shear failure and global facesheet buckling and wrinkling. Non-dimensional mass of sandwich is incorporated into failure mode maps to enable minimal weight selection. Finally, a simple procedure is proposed to utilize the developed mode maps for optimal design selection of sandwich beams with minimum weight.

Chapter 4

Structural Similitude for Sandwich Beam with Laminated Facesheet

A. S. Mondal, S. Nakhla

Faculty of Engineering and Applied Science
Memorial University of Newfoundland
St. John's, Newfoundland, Canada

An initial version of this work was published and presented in the *Canada's National Composites Conference (CANCOM 2015), Edmonton*. A version of this chapter is submitted in *Journal of Composites Part A: Applied Science and Manufacturing*. The author of this manuscript Aninda Mondal developed this work under the supervision of Dr. Sam Nakhla. Mr. Mondal's contribution to this paper is as follows:

- Performed all literature searches required for background information.
- Derived the necessary equation for the bending stiffness matrix.
- Performed all the analysis and calculations.
- Performed all the finite element analysis and constructed the necessary plots.
- Analysed the results.

- Wrote the paper.

Dr. Sam Nakhla provided continuous technical guidance and editing of the manuscript. In this chapter the manuscript is presented with altered figure numbers, table numbers and reference formats in order to match the thesis formatting guidelines set out by Memorial University.

Abstract: This study addresses the structural similitude of sandwich beams with laminated facesheet under generally applied loads. Euler-Bernoulli beam theory is used to describe the governing equation of sandwich beams with soft core. Structural similarity conditions are derived in the cases of distributed, shear and bending loads. These similarity conditions enable the design of a smaller test model from which the behavior of a larger prototype can be predicted. Finite element analysis is used to verify the derived similarity conditions and requirements. Comparisons of through the thickness stresses are obtained and found to be in excellent agreement.

Keywords: Sandwich beam, Similitude

4.1 Introduction

Since World War II the use of sandwich beams is increased in Aerospace, transportation and Marine industries. High stiffness-to-weight ratio of sandwich beams is their major advantage making to suite these industries. Meanwhile, structural components and applications in these industries are characterized by their large size. Moreover, stringent requirements are imposed on the design of these structural components for certification purposes. Certification requirements dictate testing full scale prototypes of these structural components. Full scale prototype testing represents a challenging undertaking for the designer in terms of high cost and special equipment requirements. Consequently identifying a scaled-down model of similar structural behavior to the prototype for testing purposes can provide efficient and cost effective solution. Structural similitude enables deriving similarity conditions between the prototype and the scaled-down model possessing similar behavior. Meanwhile, the high number of design parameters of sandwich beam with laminated facesheet represents a major challenge in deriving associated similarity conditions. Therefore the objective of this work is to identify the necessary constraints that allow developing these similarity conditions for a sandwich beam with laminated facesheet under variety of applied loads.

Many researchers conducted analytical, numerical and experimental studies on similitude of composite structures. Simitses [39] studied similitude of flat laminated surfaces. In his study he performed theoretical study on a small scale model of laminated surface for bending, buckling and vibration. Using scaling laws he predicted the behavior of a large-scale prototype. Simitses and Rezaeepazhand [40–42] studied

structural similitude and scaling laws for flat and cylindrical laminated plates and shells. Using matrix method, dimensional analysis and governing equation method they presented the scaling laws for laminated plates. Shokrieh and Askari [43] used sequential similitude method to study the similitude of composite laminates for impact loading and buckling loading. Frostig and Simites [25] presented similitude analysis of a sandwich unidirectional beam under compressive buckling loads. Mckown et al. [44] investigated scaling effects in fiber-metal laminates under low velocity impact. Gurvich and Pipes [45] presented results of theoretical and experimental analysis of size effect on strength of laminated composites. Qian et al. [46] conducted experimental studies for scaling laws of composite plates for impact damage. Jackson et al. [47] analyzed and conducted experimental studies for similitude analysis of composite plates in tension and flexure. Similitude for laminated tube structures were studied in [48–50]. Frostig and Simites [26] studied similitude analyze of sandwich beam. Using higher order sandwich theory they presented the necessary conditions for similarity between a model and prototype for a sandwich beam with a foam core and isotropic facesheets. In the current study, the governing differential equation based on Euler-Bernoulli beam theory is used to derive the similitude conditions for sandwich beam with laminated facesheet and soft core. Practical geometric and material guidelines are delineated from the analysis and presented as requirements on the manufacturing of scaled-down models. Finally, finite element analysis is used to verify the accuracy of derived similarity conditions and manufacturing requirements.

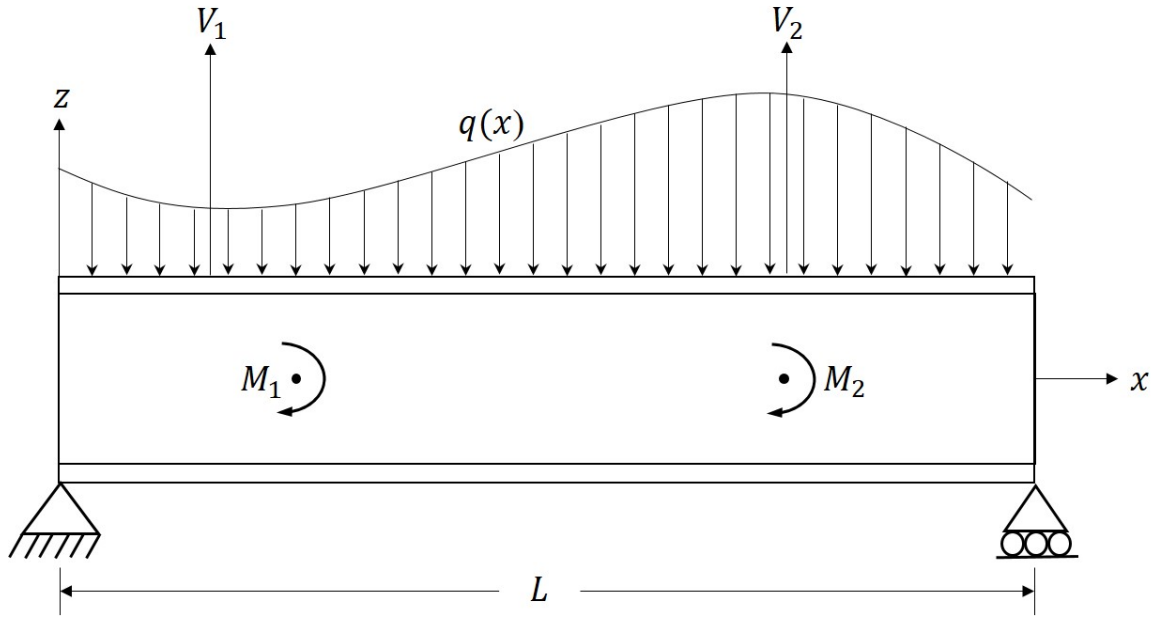


Figure 4.1: Sandwich beam subjected to a distributed load, shear load and moment

4.2 Mathematical Formulation

Considering a simply supported sandwich beam of length L and width b subjected to a distributed load $q(x)$, shear loads V_i and moments M_i as shown in Figure (4.1). In the case of distributed load $q(x)$ the governing differential equation for the beam in terms of transverse deflection $w(x)$ [3]

$$bD_{11} \frac{d^4 w}{dx^4} = q(x) \quad (4.1)$$

where, D_{11} is the bending stiffness of sandwich beam. Using similitude theory the variables in Equation (4.1) can be written as $x_p = \lambda_x x_m$. Where λ is the scale factor of variable x and the indices p and m are used to denote prototype and model,

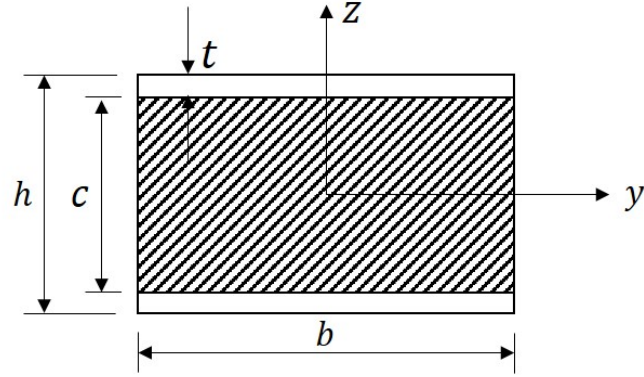


Figure 4.2: Cross section of a sandwich beam

respectively. Therefore the prototype equation can be written as

$$b_p D_{11p} \frac{d^4 w_p}{dx_p^4} = q_p \quad (4.2)$$

While the model equation is

$$b_m D_{11m} \frac{d^4 w_m}{dx_m^4} = q_m \quad (4.3)$$

The relations between geometries, stiffness properties and loading conditions of the prototype and the model in terms of the scaling factors λ 's are

$$b_p = \lambda_b b_m, D_{11p} = \lambda_D D_{11m}, w_p = \lambda_w w_m, x_p = \lambda_x x_m, q_p = \lambda_q q_m \quad (4.4)$$

Rewriting Equation (4.2) in terms of the scaling factors

$$\lambda_b b_m \lambda_D D_{11m} \frac{\lambda_w d^4 w_m}{\lambda_x^4 dx_m^4} = \lambda_q q_m \quad (4.5)$$

Dividing Equations (4.5) and (4.3) the scaling factors in the case of distributed load satisfy

$$\lambda_b \lambda_D \frac{\lambda_w}{\lambda_x^4} = \lambda_q \quad (4.6)$$

In the case the beam is subjected to transverse shear load V , the governing differential equation for the beam in terms of the transverse deflection $w(x)$ [3]

$$bD_{11} \frac{d^3 w}{dx^3} = V \quad (4.7)$$

Using the theory of similitude and similar to previous steps the scaling factors in the case of shear load satisfy

$$\lambda_b \lambda_D \frac{\lambda_w}{\lambda_x^3} = \lambda_V \quad (4.8)$$

In the case of uniform bending load M , the governing differential equation for the beam in terms of the transverse deflection $w(x)$ [3]

$$bD_{11} \frac{d^2 w}{dx^2} = M \quad (4.9)$$

Similarly the scaling factors in the case of bending moment satisfy

$$\lambda_b \lambda_D \frac{\lambda_w}{\lambda_x^2} = \lambda_M \quad (4.10)$$

Equations (4.6), (4.8) and (4.10) identify seven scale factors required to guarantee consistent behavior between the prototype and model. The scale factors belong to spatial geometry, loading, stiffness parameters of the sandwich beam. Spatial geometry scale factors are λ_b , λ_w and λ_x , load scale factors are λ_q , λ_V and λ_M and the

stiffness scale factor is λ_D . Therefore, it is necessary to further analyze the stiffness scale factor λ_D in terms of through the thickness geometry and material properties. For this purpose a symmetric sandwich beam with laminated facesheet and foam core, shown in Figure (4.3), is considered. The expression for the bending stiffness matrix \mathbf{D} can be found in [36]

$$\mathbf{D} = \frac{1}{3} \sum_{k=1}^{2n+1} \bar{Q}_k (h_k^3 - h_{k-1}^3) \quad (4.11)$$

where h_k denotes through the thickness location and \bar{Q}_k is the reduced stiffness matrix of the k -th layer or core and n is the number of layers in the facesheet. Equation (4.11) can be expanded and written as

$$\begin{aligned} \mathbf{D} = \frac{1}{3} & \left[\bar{Q}_1 (h_1^3 - h_0^3) + \bar{Q}_2 (h_2^3 - h_1^3) + \dots + \bar{Q}_k (h_k^3 - h_{k-1}^3) + \dots \right. \\ & \left. + \bar{Q}_n (h_n^3 - h_{n-1}^3) + \bar{Q}_c (h_{n+1}^3 - h_n^3) + \dots + \bar{Q}_{2n+1} (h_{2n+1}^3 - h_{2n}^3) \right] \end{aligned} \quad (4.12)$$

Assuming all layers in facesheet are of equal thickness t_l , Equation (4.12) can be further simplified and written in terms of total thickness of the facesheet t , core thickness c , and the number of layers in the facesheet n .

$$\begin{aligned} \mathbf{D} = \frac{1}{2} c^2 t_l \sum_{k=1}^n \bar{Q}_k + 2ctt_l \sum_{k=1}^n \bar{Q}_k + 2t^2 t_l \sum_{k=1}^n \bar{Q}_k + \frac{2}{3} t^3 \sum_{k=1}^n \bar{Q}_k (3k^2 - 3k + 1) \\ - ct_l^2 \sum_{k=1}^n \bar{Q}_k (2k - 1) - 2tt_l^2 \sum_{k=1}^n \bar{Q}_k (2k - 1) - \frac{1}{12} \bar{Q}_c c^3 \end{aligned} \quad (4.13)$$

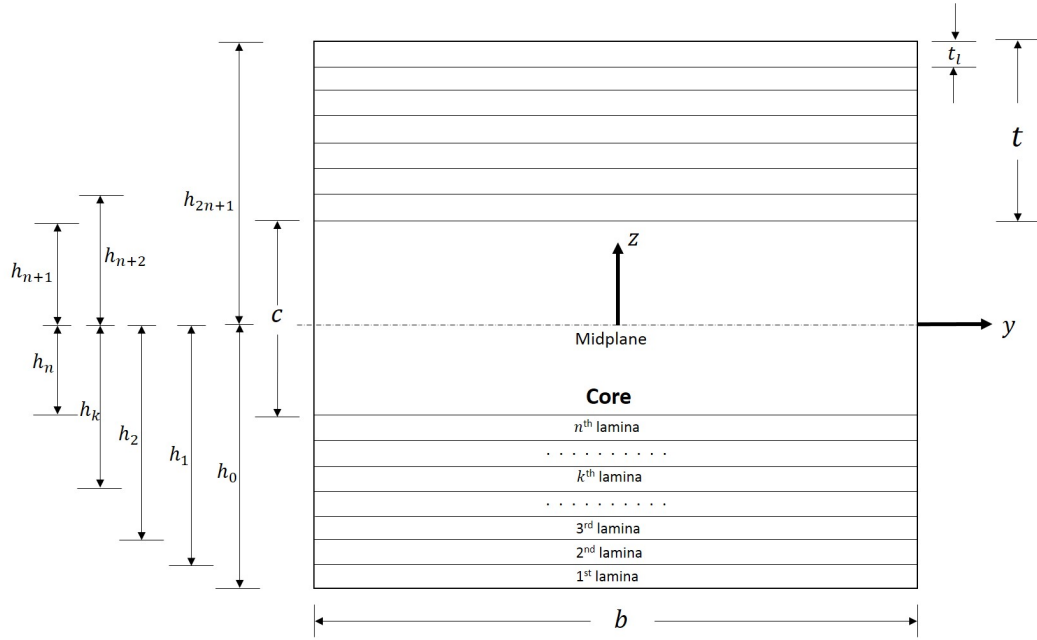


Figure 4.3: Cross-sectional geometry of a laminate sandwich beam

Therefore,

$$\begin{aligned}
 D_{11} = & \frac{1}{2}c^2t_l \sum_{k=1}^n \bar{Q}_{11k} + 2ctt_l \sum_{k=1}^n \bar{Q}_{11k} + 2t^2t_l \sum_{k=1}^n \bar{Q}_{11k} + \frac{2}{3}t^3 \sum_{k=1}^n \bar{Q}_{11k}(3k^2 - 3k + 1) \\
 & - ct_l^2 \sum_{k=1}^n \bar{Q}_{11k}(2k - 1) - 2tt_l^2 \sum_{k=1}^n \bar{Q}_{11k}(2k - 1) - \frac{1}{12}\bar{Q}_{11c}c^3
 \end{aligned} \tag{4.14}$$

Equation (4.14) can be written for prototype as

$$\begin{aligned}
 D_{11p} = & \frac{1}{2}c_p^2t_{lp} \sum_{k=1}^{n_p} \bar{Q}_{11k_p} + 2c_p t_p t_{lp} \sum_{k=1}^{n_p} \bar{Q}_{11k_p} + 2t_p^2 t_{lp} \sum_{k=1}^{n_p} \bar{Q}_{11k_p} + \\
 & \frac{2}{3}t_{lp}^3 \sum_{k=1}^{n_p} \bar{Q}_{11k_p}(3k^2 - 3k + 1) - c_p t_{lp}^2 \sum_{k=1}^{n_p} \bar{Q}_{11k_p}(2k - 1) \\
 & - 2t_p t_{lp}^2 \sum_{k=1}^{n_p} \bar{Q}_{11k_p}(2k - 1) - \frac{1}{12}\bar{Q}_{11c_p}c_p^3
 \end{aligned} \tag{4.15}$$

and for the model as

$$\begin{aligned}
D_{11m} = & \frac{1}{2}c_m^2 t_{l_m} \sum_{k=1}^{n_m} \bar{Q}_{11k_m} + 2c_m t_m t_{l_m} \sum_{k=1}^{n_m} \bar{Q}_{11k_m} + 2t_m^2 t_{l_m} \sum_{k=1}^{n_m} \bar{Q}_{11k_m} + \\
& \frac{2}{3}t_{l_m}^3 \sum_{k=1}^{n_m} \bar{Q}_{11k_m} (3k^2 - 3k + 1) - c_m t_{l_m}^2 \sum_{k=1}^{n_m} \bar{Q}_{11k_m} (2k - 1) \\
& - 2t_m t_{l_m}^2 \sum_{k=1}^{n_m} \bar{Q}_{11k_m} (2k - 1) - \frac{1}{12} \bar{Q}_{11c_m} c_m^3
\end{aligned} \quad (4.16)$$

Identifying through-the-thickness scale factors

$$t_{l_p} = \lambda_{t_l} t_{l_m}, c_p = \lambda_c c_m, t_p = \lambda_t t_m, \sum_{k=1}^{n_p} \bar{Q}_{11k_p} = \lambda_{\Sigma \bar{Q}} \sum_{k=1}^{n_m} \bar{Q}_{11k_m} \text{ and } \bar{Q}_{c_p} = \lambda_{\bar{Q}_c} \bar{Q}_{c_m} \quad (4.17)$$

After dividing Equation(4.15) with Equation(4.16) the following scaling ratios exists

$$\begin{aligned}
\lambda_D = & \frac{c_p^2 t_{l_p} \sum_{k=1}^{n_p} \bar{Q}_{11k_p}}{c_m^2 t_{l_m} \sum_{k=1}^{n_m} \bar{Q}_{11k_m}} = \frac{c_p t_p t_{l_p} \sum_{k=1}^{n_p} \bar{Q}_{11k_p}}{c_m t_m t_{l_m} \sum_{k=1}^{n_m} \bar{Q}_{11k_m}} = \frac{t_p^2 t_{l_p} \sum_{k=1}^{n_p} \bar{Q}_{11k_p}}{t_m^2 t_{l_m} \sum_{k=1}^{n_m} \bar{Q}_{11k_m}} \\
= & \frac{t_{l_p}^3 \sum_{k=1}^{n_p} \bar{Q}_{11k_p} (3k^2 - 3k + 1)}{t_{l_m}^3 \sum_{k=1}^{n_m} \bar{Q}_{11k_m} (3k^2 - 3k + 1)} = \frac{c_p t_{l_p}^2 \sum_{k=1}^{n_p} \bar{Q}_{11k_p} (2k - 1)}{c_m t_{l_m}^2 \sum_{k=1}^{n_m} \bar{Q}_{11k_m} (2k - 1)} \\
= & \frac{t_p t_{l_p}^2 \sum_{k=1}^{n_p} \bar{Q}_{11k_p} (2k - 1)}{t_m t_{l_m}^2 \sum_{k=1}^{n_m} \bar{Q}_{11k_m} (2k - 1)} = \frac{\bar{Q}_{11c_p} c_p^3}{\bar{Q}_{11c_m} c_m^3}
\end{aligned} \quad (4.18)$$

Using the relations provided in Equation (4.17) into Equations (4.18) the following conditions are realized

$$\lambda_D = \lambda_c^2 \lambda_{t_l} \lambda_{\Sigma \bar{Q}} = \lambda_c \lambda_{t_l} \lambda_t \lambda_{\Sigma \bar{Q}} = \lambda_t^2 \lambda_{t_l} \lambda_{\Sigma \bar{Q}} = \lambda_{\bar{Q}_c} \lambda_c^3 \quad (4.19)$$

Originally the stiffness scale factor λ_D is identified as one of seven scale factors of the problem. Using Equation (4.19) λ_D can be replaced by five scale factor, namely, λ_c , λ_t , λ_{t_l} , $\lambda_{\bar{Q}_c}$ and $\lambda_{\Sigma \bar{Q}}$. Consequently, a total of eleven scale factors are necessary and

sufficient to correlate the model behavior to the prototype. These scale factors are required to satisfy seven equations, namely, Equations (4.6), (4.8), (4.10) and (4.19). Therefore, four conditions are required to be imposed to the problem to uniquely determine the scale factors. These conditions are mainly dictated by manufacturing requirements. It is intuitive to use the same material of the prototype to build the model. For example, using the same foam material for the core and same prepreg layers for the facesheet. It is also necessary to maintain identical stacking sequence for the facesheet in the model as the prototype. On the other hand, no conditions are imposed on the total thickness of the model; it needs to be determined from equations. Imposing these conditions of identical materials and stacking sequence in the facesheet result in

$$\lambda_{t_l} = \frac{t_{l_p}}{t_{l_m}} = 1 \quad (4.20)$$

and

$$\lambda_{\bar{Q}_c} = 1 \quad (4.21)$$

Whereas,

$$\lambda_t = \frac{t_p}{t_m} = \frac{n_p t_{l_p}}{n_m t_{l_m}} = \frac{n_p}{n_m} = \lambda_n \quad (4.22)$$

Which leads to the scale factor of total sum of reduced stiffness matrix of the facesheet,

$$\lambda_{\Sigma \bar{Q}} = \frac{\sum_{k=1}^{n_p} \bar{Q}_{11k_p}}{\sum_{k=1}^{n_m} \bar{Q}_{11k_m}} = \lambda_n \quad (4.23)$$

Substituting the relations in Equations (4.20), (4.21), (4.22) and (4.23) into (4.19)

$$\lambda_D = \lambda_c^2 \lambda_n = \lambda_c \lambda_n^2 = \lambda_n^3 = \lambda_c^3 \quad (4.24)$$

Equation (4.24) dictates equality of scale factors

$$\lambda_c = \lambda_n \quad (4.25)$$

Inspecting Equations (4.22), (4.23) and (4.25) scale factors λ_t , λ_c , $\lambda_{\Sigma \bar{Q}}$ and consequently λ_D can be expressed using only one scale factor λ_c . Rewriting Equations (4.6), (4.8) and (4.10) in terms of these conditions

$$\lambda_b \lambda_n^3 \frac{\lambda_w}{\lambda_x^4} = \lambda_q \quad (4.26)$$

$$\lambda_b \lambda_n^3 \frac{\lambda_w}{\lambda_x^3} = \lambda_V \quad (4.27)$$

$$\lambda_b \lambda_n^3 \frac{\lambda_w}{\lambda_x^2} = \lambda_M \quad (4.28)$$

Scale factors λ_b , λ_x and λ_n define the geometric scaling between the prototype and model. Therefore imposing uniform geometric scaling, $\lambda_b = \lambda_x = \lambda_n$ results in

$$\frac{\lambda_b}{\lambda_n} \frac{\lambda_w}{\lambda_n} \frac{\lambda_n^4}{\lambda_x^4} = \frac{\lambda_q}{\lambda_n} \quad (4.29)$$

$$\frac{\lambda_b}{\lambda_n} \frac{\lambda_w}{\lambda_n} \frac{\lambda_n^3}{\lambda_x^3} = \frac{\lambda_V}{\lambda_n^2} \quad (4.30)$$

$$\frac{\lambda_b}{\lambda_n} \frac{\lambda_w}{\lambda_n} \frac{\lambda_n^2}{\lambda_x^2} = \frac{\lambda_M}{\lambda_n^3} \quad (4.31)$$

Which in turn imposes these scale factors to the applied load

$$\lambda_q = \lambda_n, \lambda_V = \lambda_n^2, \lambda_M = \lambda_n^3 \quad (4.32)$$

In conclusion, imposing conditions on manufacturing requirements using the same materials and facesheet stacking sequence and performing uniform scaling in spatial and thickness directions are the necessary and sufficient conditions to identify the applied load scale factors.

4.3 Numerical Analysis and Comparison with Experiments

Finite element analysis is used to investigate the accuracy of scale parameters developed within. ABAQUS v6.11 commercial finite element software is used for this purpose. Three problems are considered for validation purposes, namely, simply supported beam under uniformly distributed load, three-point bending and four-point bending. In each case the geometry and materials of the test specimen(model) is outlined and a corresponding prototype specifications are obtained using derived scales. Through-the-thickness normal and shear stresses in the models are compared to corresponding values in prototypes.

4.3.1 Sandwich beam under uniformly distributed load

In this section, a simply supported sandwich beam under uniformly distributed load is proposed to evaluate the accuracy of the distributed load scale factor. The sandwich beam is composed of T-300 carbon-epoxy facesheets with total of 80 layers in $[0/90]_s$ and a phenolic foam core. Material properties of carbon-epoxy and phenolic foam are obtained from Mallick [36] and Manalo [51], respectively, and are provided in Table

4.1.

Table 4.1: Material properties of sandwich beam in distributed loading

Part	Material	E_1 (GPa)	E_2 (GPa)	ν_{12}	G_{12} (GPa)	G_{13} (GPa)	G_{23} (GPa)
Facesheet	Carbon/Epoxy T-300	133.44	8.78	0.26	3.254	3.254	3.2631
Core	Phenolic Foam	1.32	-	0.29	-	-	-

An assumed prototype sandwich beam is 2 m long, 0.3 m wide and thicknesses of facesheet and core are 0.012 m and 0.16 m, respectively. The applied uniformly distributed load is of intensity $q_p = 3500$ N/m. A uniform geometric scaling of $\lambda_n = 10$ is used to obtain the geometry of a model of suitable size for testing. Hence, the uniform distributed load to the model maintains λ_n ratio with that applied to prototype; $q_m = 350$ N/m. The facesheet in the model will be 8 layers in $[0/90]_s$. The model length is 0.2 m, width is 0.03 m and thickness of the facesheet and core are 1.2 mm and 16 mm, respectively. Both the model and the prototype are analysed in ABAQUS for the purpose of comparing through-the-thickness normal and shear stresses. The sandwich beam is modeled as three dimensional deformable shell discretized into a spatial mesh of 100×20 four-noded, reduced integration doubly curved shell elements S4R. S4R is a 4-node, quadrilateral, stress/displacement shell element with reduced integration and a large-strain formulation. The shell section is defined according to provided stacking sequence of facesheet and respective thickness of facesheet and core. Normal and shear stresses through-the-thickness are obtained for the prototype and model and shown in Figures 4.4 and 4.5, respectively, in terms

of the non-dimensional thickness. It can be noticed that normal and shear stress predictions in the prototype and the model are in perfect agreement.

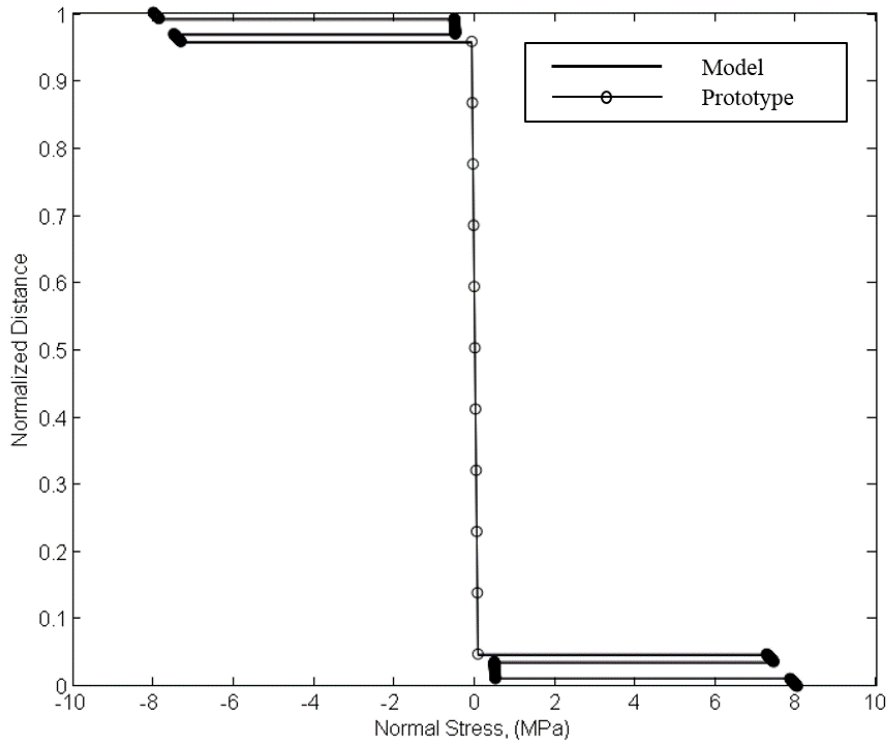


Figure 4.4: Normal stress distribution through the normalized thickness of model and prototype for distributed loading

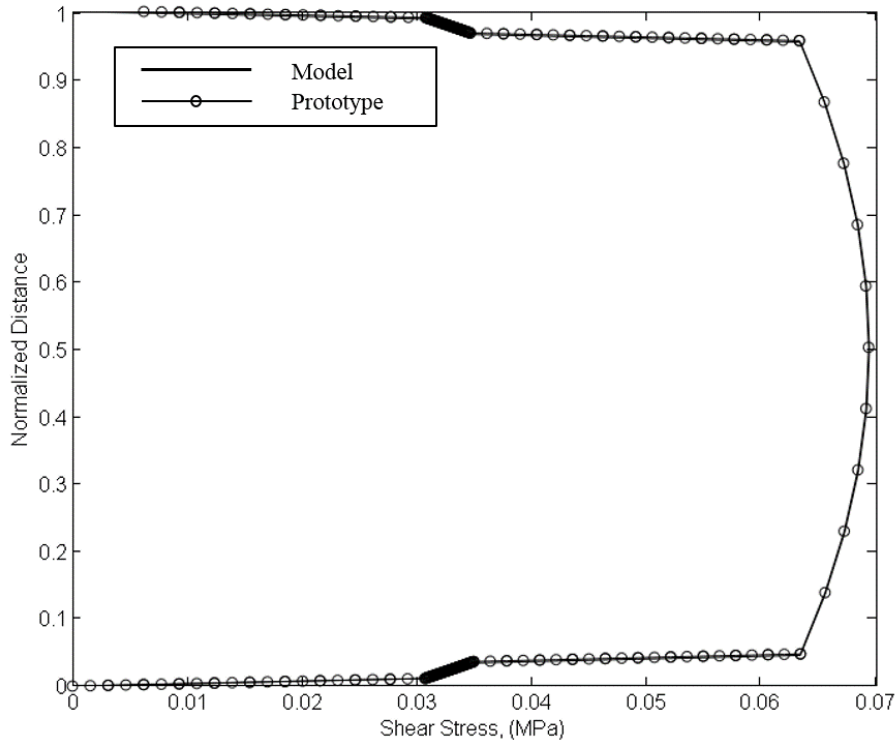


Figure 4.5: Shear stress distribution through the normalized thickness of model and prototype for distributed loading

4.3.2 Comparison with three-point bending test

In this section, a three-point bending test is chosen from literature [51] to investigate the accuracy of the derived scaling laws in the case of shear load. In the three-point bending test conducted by Manalo [51] the sandwich beam is composed of 10 layers of Bi-axial [0/90] E-CR glass fibre facesheets and phenolic foam core. The obtained properties of E-CR facesheet and phenolic foam core are provided in Table 4.2 [52]. The specimen length is 0.24 m, width is 0.05 m and thickness of the facesheet and core are 3 mm and 14 mm, respectively. The observed failure mode of the sandwich

beam from the three-point bending test is shear crack in the core and the failure load occurred at $V_m = 8.83$ KN. For a uniform geometric scaling of $\lambda_n = 10$ the prototype length is 2.4 m, width is 0.5 m and thicknesses of the facesheet and core are 30 mm and 140 mm, respectively. Equation (4.32) predicts that the prototype should experience failure at $V_p = \lambda_n^2 V_m = 883$ kN. Both the model and the prototype are analysed in ABAQUS for the purpose of comparing through-the-thickness maximum shear stresses. The sandwich beam is modeled as three dimensional deformable shell discretized into a spatial mesh of 100×20 four-noded, reduced integration doubly curved shell elements S4R. The shell section is defined according to the stacking sequence of facesheet and respective thickness of facesheet and core. Shear stresses through the thickness are obtained for the prototype and model and shown in Figure 4.6 in terms of non-dimensional thickness. It can be noticed that shear stress predictions in the prototype and the model are in perfect agreement.

Table 4.2: Material properties of sandwich beam used in 3-point bending test [51, 52]

Part	Material	E_1 (GPa)	E_2 (GPa)	ν_{12}	G_{12} (GPa)	G_{13} (GPa)	G_{23} (GPa)
Facesheet	E-CR Glass Fiber	14.284	3.664	0.25	2.466	2.466	1.396
Core	Phenolic Foam	1.32	-	0.29	-	-	-

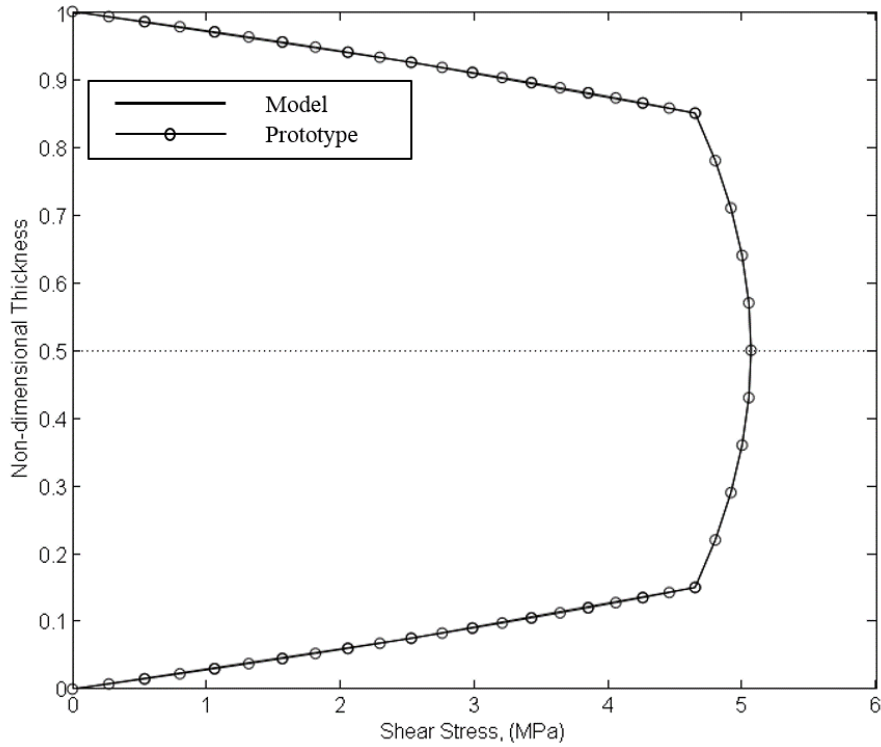


Figure 4.6: Shear stress distribution through the normalized thickness of model and prototype for shear loading

4.3.3 Comparison with four-point bending test

In this section a four-point bending test is chosen from literature [53] to investigate the accuracy of the derived scaling laws in the case of applied moment. In [53] they tested a number of flat and curved sandwich beams with soft core to investigate the effect of facesheet debonding on their free vibration response. For this purpose they conducted a four-point bending static test of a flat sandwich beam and documented the load of failure or debonding. In this four-point bending test the sandwich beam is composed of carbon/epoxy facesheets and polyurethane foam core. The properties

of carbon/epoxy facesheet and polyurethane foam core are provided in Table 4.3.

Table 4.3: Material properties of sandwich beam used in 4-point bending test [53]

Part	Material	E_1 (GPa)	E_2 (GPa)	ν_{12}	G_{12} (GPa)	G_{13} (GPa)	G_{23} (GPa)
Facesheet	Carbon/Epoxy	10.658	10.658	0.26	4.0	4.0	4.0
Core	Polyurethane Foam	115	-	0.3	-	-	-

The beam length is $L_m = 0.254$ m, width is $b_m = 0.0254$ m and thicknesses of the facesheet and core are, 0.762 mm and 12.7 mm, respectively. The support span length is 120mm and loading span is 40 mm. They [53] documented the initial failure of the sandwich beam taking place at peak load of 715 N. Therefore the maximum moment applied to the beam is $M_m = 14.3$ Nm. For a uniform geometric scaling of $\lambda_n = 10$ the prototype length is 2.54 m, width is 0.254 m and thicknesses of the facesheet and core are 7.62 mm and 127 mm, respectively. Equation (4.32) predicts that the prototype should experience failure at $M_p = \lambda_n^3 M_m = 14300$ Nm. Both the model and the prototype are analysed in ABAQUS for the purpose of comparing through-the-thickness maximum shear stresses. The sandwich beam is modeled as three dimensional deformable shell discretized into a spatial mesh of 100*20 four-noded, reduced integration doubly curved shell elements S4R. The shell section is defined according to stacking sequence of facesheet and respective thickness of facesheet and core. Normal stresses through the thickness are obtained for the prototype and model and shown in Figure 4.7 in terms of non-dimensional thickness. It can be noticed that normal stress predictions in the prototype and the

model are in perfect agreement.

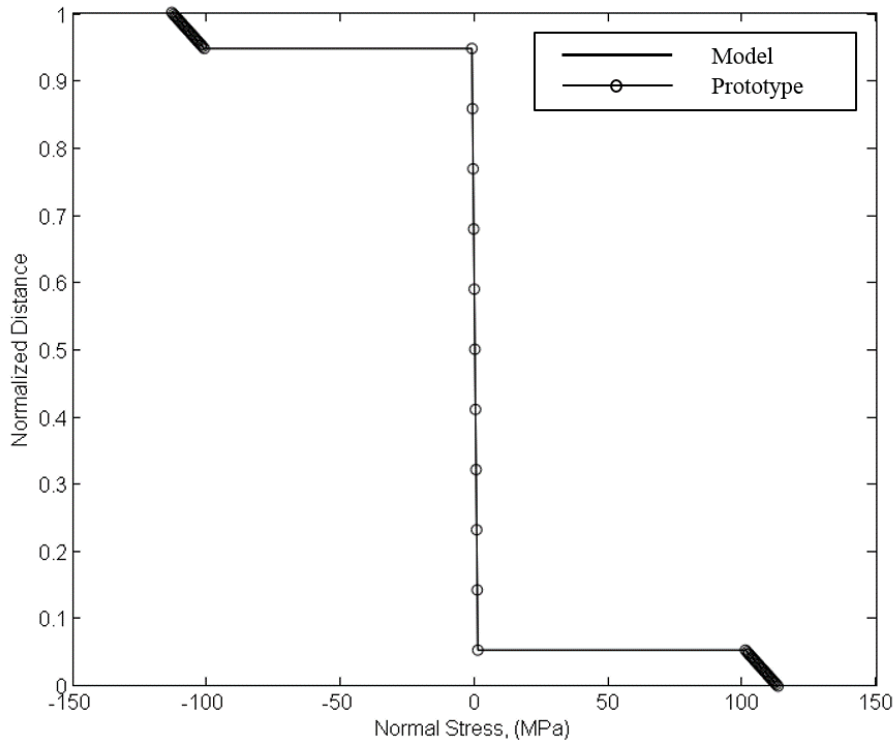


Figure 4.7: Normal stress distribution through the normalized thickness of model and prototype for applied moment

4.4 Discussion and Conclusion

In this paper, similarity conditions were developed for a symmetric sandwich beam with laminated composite facesheets and a foam core where the beam was subjected to bending. The foam core was assumed to be isotropic. The analysis was performed using simple beam theory and classical lamination theory. Similitude conditions were developed using the governing equation of the system. The scale factor λ_n was selected

as the independent parameter. By deciding upon a certain value of scale factor λ_n , the scale factor of all the other parameters can be known. The derived similitude rules and conditions were tested and verified using finite element analysis. Real experiments done in literature were modeled in finite element tool ABAQUS. The stress distributions of both the small sandwich beam and the scaled up sandwich beam were proven to be identical. Similitude conditions allow the designer to identify the model size and loading conversion rules. Hence when testing the model and identifying its failure load the current derived rules can be used to predict failure load of the prototype. For future work experimental measurements will be obtained for the purpose of comparison with the theoretical and numerical predictions. The similitude analysis presented is a useful design tool as the similitude conditions found from this study is simple and straight forward.

Chapter 5

Conclusion

This chapter consists of a review of the main contributions of this thesis, followed by an outlook on future work.

5.1 Review

The current thesis consists of two papers those are submitted for journal publication. The current thesis discusses about designing of composite sandwich beams for offshore purposes. In Chapter 1 advantages of composite sandwich beam are explained. In spite of having good advantages over conventional materials composites are still not popular in building offshore structures. The possible reason for this is that it is still believed that composites are more expensive than conventional materials. An unoptimised design of composites may lead to higher cost. Therefore it is necessary to develop an optimisation design tool for composites. From literature review in Chapter 2 it is found that many researchers conducted tests and performed analytical studies on composite sandwich beams. They used higher order and complicated

theories and methods to formulate design tools for sandwich beams. The focus of Chapter 3 is designing of optimized sandwich beams. Simple theories are used for developing the equations. Four failure modes are selected for the analysis. It is identified that the facesheet of a sandwich beam may fail due to normal stresses, global buckling and wrinkling whereas the foam core may fail due to shear. Analytical expressions for these failure modes are introduced using simple theories and compared with corresponding established expressions. It is concluded that the expressions using simple theories give accurate enough results for the sake of design purposes. The main contribution of this chapter is introducing a new expression for the facesheet wrinkling. The expression is established by using E-B beam and PMTPE theories. The established expression is compared with four other expressions for wrinkling already established in literature. It is shown that the new approach can predict the wrinkling of the facesheet with acceptable accuracy. The expressions for the failure modes are later non-dimensionalized. An advantage of non-dimensionalization is that nondimensionalization can reveal characteristic properties of a system. These non-dimensional form of the equations are used to construct characteristic failure mode maps. Data from experiments conducted in literature is taken and used in constructing the failure mode maps. Using the failure mode maps it is shown how an optimized sandwich beam can be designed. The failure maps show that wrinkling failure is more likely to occur than global buckling of the facesheet. The failure mode maps provide which type of materials should be used. Also they provide safe zones from which the dimensions of the constituents of a sandwich beam can be selected. As sandwich beams require to be strong and also light, mass optimisation is also incorporated in the design. It is a simple tool with which any size of sandwich beam

can be designed.

After designing is complete it is necessary to manufacture and test the beams before it can be used in the original structure. Testing of original structure is not always feasible and maybe expensive to do so in most cases. Therefore similitude study of composite sandwich beams is done in Chapter 4. Similitude study of composite sandwich beams is done for three loading conditions, distributed load, shear load and moment load. The study is done using governing equation method. The reason for choosing this method is that a governing equation is same for any system regarding the size of the system. From analysis eleven unknown variables are identified. Using practical manufacturing conditionis and constraints all these unknown variables are expressed with a single known scale factor. The ratio of the number of layers between the prototype and model is selected as the known scale factor. From analysis it is found that the relation between the known scale factor and the dimensional scale factors is linear. The distributed load, shear load and moment scale factors have linear, quadratic and cubic relation with the known scale factor, respectively. From the developed similitude conditions it is possible to test a small scale specimen and by analyzing the failure mode of the small scale model failure mode of the large scale prototype can be predicted. To verify the similitude conditions a three point bending test and a four point bending test are selected from literature and they are modeled in finite element tool ABAQUS. Using the developed similitude conditions larger versions of these tests are also modeled in ABAQUS. Stress distributions through the thickness of the beams are plotted and it is found that the stress distributions between the small scale model and large scale prototype are identical. The similitude conditions developed in this chapter can be used for conducting cost effective and

feasible testing of sandwich beams.

5.2 Future Work

The analytical results found from the current study are compared with results from literature. Developed conditions are verified by finite element analysis. For future work the results developed in this work can be compared with experimental work. Sandwich beams can be designed and constructed using the design tools and experimental studies can be done. Also different sizes of sandwich beams maybe constructed using the similitude conditions developed in this work and experimental study can be conducted for further verification.

Bibliography

- [1] Scott RJ, Sommella JH. Feasibility Study of Glass Reinforced Plastic Cargo Ship. DTIC Document; 1971.
- [2] Plantema FJ. Sandwich construction. Wiley, New York; 1966.
- [3] Vinson JR. The behavior of sandwich structures of isotropic and composite materials. CRC Press; 1999.
- [4] Kim J, Swanson SR. Design of sandwich structures for concentrated loading. *Composite Structures*. 2001;52(3):365–373.
- [5] Tagarielli V, Fleck N, Deshpande V. Collapse of clamped and simply supported composite sandwich beams in three-point bending. *Composites Part B: Engineering*. 2004;35(6):523–534.
- [6] Kabir K, Vodenitcharova T, Hoffman M. Response of aluminium foam-cored sandwich panels to bending load. *Composites Part B: Engineering*. 2014;64:24–32.
- [7] McCormack T, Miller R, Kesler O, Gibson L. Failure of sandwich beams

- with metallic foam cores. *International Journal of Solids and Structures*. 2001;38(28):4901–4920.
- [8] Yu J, Wang X, Wei Z, Wang E. Deformation and failure mechanism of dynamically loaded sandwich beams with aluminum-foam core. *International Journal of Impact Engineering*. 2003;28(3):331–347.
- [9] Steeves CA, Fleck NA. Material selection in sandwich beam construction. *Scripta materialia*. 2004;50(10):1335–1339.
- [10] Chen C, Harte A, Fleck N. The plastic collapse of sandwich beams with a metallic foam core. *International Journal of Mechanical Sciences*. 2001;43(6):1483–1506.
- [11] Mohan K, Hon YT, Idapalapati S, Seow HP. Failure of sandwich beams consisting of alumina face sheet and aluminum foam core in bending. *Materials Science and Engineering: A*. 2005;409(1):292–301.
- [12] Sokolinsky VS, Shen H, Vaikhanski L, Nutt SR. Experimental and analytical study of nonlinear bending response of sandwich beams. *Composite Structures*. 2003;60(2):219–229.
- [13] Roberts J, Boyle M, Wienhold P, White G. Buckling, collapse and failure analysis of FRP sandwich panels. *Composites Part B: Engineering*. 2002;33(4):315–324.
- [14] Muc A, Zuchara P. Buckling and failure analysis of FRP faced sandwich plates. *Composite structures*. 2000;48(1):145–150.
- [15] Stiftinger MA, Rammerstorfer FG. Face layer wrinkling in sandwich shellstheo-

- retical and experimental investigations. *Thin-Walled Structures*. 1997;29(1):113–127.
- [16] Saoud KS, Le Grogne P. A unified formulation for the biaxial local and global buckling analysis of sandwich panels. *Thin-Walled Structures*. 2014;82:13–23.
- [17] Douville MA, Le Grogne P. Exact analytical solutions for the local and global buckling of sandwich beam-columns under various loadings. *International Journal of Solids and Structures*. 2013;50(16):2597–2609.
- [18] Léotoing L, Drapier S, Vautrin A. First applications of a novel unified model for global and local buckling of sandwich columns. *European Journal of Mechanics-A/Solids*. 2002;21(4):683–701.
- [19] Jasion P, Magnucka-Blandzi E, Szyc W, Magnucki K. Global and local buckling of sandwich circular and beam-rectangular plates with metal foam core. *Thin-Walled Structures*. 2012;61:154–161.
- [20] Østergaard RC. Buckling driven debonding in sandwich columns. *International Journal of Solids and Structures*. 2008;45(5):1264–1282.
- [21] Wu HC, Mu B, Warnemuende K. Failure analysis of FRP sandwich bus panels by finite element method. *Composites Part B: Engineering*. 2003;34(1):51–58.
- [22] Pokharel N, Mahendran M. Finite element analysis and design of sandwich panels subject to local buckling effects. *Thin-walled structures*. 2004;42(4):589–611.
- [23] Awad ZK, Aravinthan T, Zhuge Y. Experimental and numerical analysis of an

- innovative GFRP sandwich floor panel under point load. *Engineering Structures*. 2012;41:126–135.
- [24] Bambal AS. Mechanical evaluation and FE modeling of composite sandwich panels. ProQuest; 2007.
- [25] Frostig Y, Simitzes G. Similitude of sandwich panels with a softcore in buckling. *Composites Part B: Engineering*. 2004;35(6):599–608.
- [26] Frostig Y, Simitzes G. Structural similitude and scaling laws for sandwich beams. *AIAA journal*. 2002;40(4):765–773.
- [27] Allen HG. *Analysis and Design of Structural Sandwich Panels: The Commonwealth and International Library: Structures and Solid Body Mechanics Division*. Elsevier; 2013.
- [28] Carlsson LA, Kardomateas GA. *Structural and failure mechanics of sandwich composites*. vol. 121. Springer Science & Business Media; 2011.
- [29] Niu K, Talreja R. Modeling of wrinkling in sandwich panels under compression. *Journal of Engineering Mechanics*. 1999;125(8):875–883.
- [30] Mondal A, Nakhla S. Simplified model for the design of composite sandwich construction. In: *Oceans-St. John's, 2014. IEEE*; 2014. p. 1–12.
- [31] Daniel I, Gdoutos E, Wang KA, Abot J. Failure modes of composite sandwich beams. *International Journal of Damage Mechanics*. 2002;11(4):309–334.
- [32] Petras A, Sutcliffe M. Failure mode maps for honeycomb sandwich panels. *Composite Structures*. 1999;44(4):237–252.

- [33] Shenhar Y, Frostig Y, Altus E. Stresses and failure patterns in the bending of sandwich beams with transversely flexible cores and laminated composite skins. *Composite Structures*. 1996;35(2):143–152.
- [34] Steeves CA, Fleck NA. Collapse mechanisms of sandwich beams with composite faces and a foam core, loaded in three-point bending. Part I: analytical models and minimum weight design. *International Journal of Mechanical Sciences*. 2004;46(4):561–583.
- [35] Gere J, Goodno B. *Mechanics of materials*. Nelson Education; 2012.
- [36] Mallick PK. *Fiber-reinforced composites: materials, manufacturing, and design*. CRC press; 2007.
- [37] Chiras S, Mumm D, Evans A, Wicks N, Hutchinson J, Dharmasena K, et al. The structural performance of near-optimized truss core panels. *International Journal of Solids and Structures*. 2002;39(15):4093–4115.
- [38] Bauchau OA, Craig JJ. *Structural analysis: with applications to aerospace structures*. vol. 163. Springer Science & Business Media; 2009.
- [39] Simitse GJ. Structural similitude for flat laminated surfaces. *Composite structures*. 2001;51(2):191–194.
- [40] Simitse G, Starnes Jr J, Rezaeepazhand J. Structural similitude and scaling laws for plates and shells: a review. In: *Advances in the Mechanics of Plates and Shells*. Springer; 2002. p. 295–310.

- [41] Simitse GJ, Rezaeepazhand J. Structural Similitude and Scaling Laws for Laminated Beam-Plates. NASA-Langley Research Center, Hampton, Virginia; 1992.
- [42] Rezaeepazhand J. Structural similitude and scaling laws for laminated cylindrical shells and panels [Ph.D. Thesis]. University of Cincinnati. Cincinnati, OH, United States; 1995.
- [43] Shokrieh M, Askari A. Similitude Study of Impacted Composite Laminates under Buckling Loading. *Journal of Engineering Mechanics*. 2012;139(10):1334–1340.
- [44] McKown S, Cantwell W, Jones N. Investigation of scaling effects in fibermetal laminates. *Journal of composite materials*. 2008;42(9):865–888.
- [45] Gurvich MR, Pipes RB. Strength size effect of laminated composites. *Composites science and technology*. 1995;55(1):93–105.
- [46] Qian Y, Swanson S, Nuismer R, Bucinell R. An experimental study of scaling rules for impact damage in fiber composites. *Journal of Composite Materials*. 1990;24(5):559–570.
- [47] Jackson KE, Kellas S, Morton J. Scale effects in the response and failure of fiber reinforced composite laminates loaded in tension and in flexure. *Journal of composite materials*. 1992;26(18):2674–2705.
- [48] Tarfaoui M, Gning PB, Davies P, Collombet F. Scale and size effects on dynamic response and damage of glass/epoxy tubular structures. *Journal of composite materials*. 2007;41(5):547–558.

- [49] Derisi B, Hoa S, Hojjati M. Similitude study on bending stiffness and behavior of composite tubes. *Journal of Composite Materials*. 2012;p. 0021998311431642.
- [50] Chouchaoui C, Ochoa O. Similitude study for a laminated cylindrical tube under tensile, torsion, bending, internal and external pressure. Part I: governing equations. *Composite Structures*. 1999;44(4):221–229.
- [51] Manalo A. Behaviour of fibre composite sandwich structures under short and asymmetrical beam shear tests. *Composite Structures*. 2013;99:339–349.
- [52] Manalo A, Aravinthan T, Karunasena W, Islam M. Flexural behaviour of structural fibre composite sandwich beams in flatwise and edgewise positions. *Composite Structures*. 2010;92(4):984–995.
- [53] Baba BO, Thoppul S. An experimental investigation of free vibration response of curved sandwich beam with face/core debond. *Journal of Reinforced Plastics and Composites*. 2010;29(21):3208–3218.

Appendix A

Non-dimensionalisation of Analytical Expressions

In this chapter the non-dimensionalisation procedure of the analytical expressions used in chapter 3 is explained.

A.1 Normal Stress

The facesheets of a sandwich beam carries the normal stresses while the sandwich beam is subjected to bending. Maximum normal stress acts at the top and bottom edge of the sandwich panel. Maximum normal stress in the facesheet can be predicted using the following expression

$$\sigma_f = \frac{E_f M (h/2)}{E_f I_f + E_c I_c} \quad (\text{A.1})$$

Equation (A.1) can be rewritten as

$$\sigma_f = M \frac{h/2}{I_f + \bar{E}I_c} \quad (\text{A.2})$$

where, $\bar{E} = E_c/E_f$ The non-dimensional normal stress $\bar{\sigma}$ is defined as

$$\bar{\sigma} = \sigma_f / \sigma_{allw} \quad (\text{A.3})$$

where, σ_{allw} is the allowable normal stress in the facesheet. Substituting σ_f from Equation (A.2) into Equation (A.3)

$$\bar{\sigma} = \frac{M}{\sigma_{allw}} \frac{h/2}{I_f + \bar{E}I_c} \quad (\text{A.4})$$

Introducing the non-dimensional moment \bar{M} in Equation (A.4)

$$\bar{\sigma} = \bar{M} \frac{btd}{2} \frac{h/2}{I_f + \bar{E}I_c} \quad (\text{A.5})$$

The second moment of area of the facesheets can be written as

$$I_f = \frac{btd^2}{2} \quad (\text{A.6})$$

The second moment of area of the core can be written as

$$I_c = \frac{bc^3}{12} \quad (\text{A.7})$$

Substituting the expressions from Equation (A.6) and Equation (A.7) into Equation (A.5)

$$\bar{\sigma} = \bar{M} \frac{3htd}{6td^2 + \bar{E}c^3} \quad (\text{A.8})$$

Introducing the non-dimensional geometrical parameters \bar{t} and \bar{c} in Equation (A.8)

$$\bar{\sigma} = \bar{M} \frac{3\bar{t}(\bar{c} + \bar{t})}{6\bar{t}(\bar{c} + \bar{t})^2 + \bar{E}\bar{c}^3} \quad (\text{A.9})$$

A.2 Shear Stress

Maximum shear stress in the core can be predicted using the following expression

$$\tau_c = \frac{V}{EI_{eq}} \left(\frac{E_f t d}{2} + \frac{E_c c^2}{8} \right) \quad (\text{A.10})$$

The total bending rigidity of the sandwich beam can be written as

$$EI_{eq} \approx \frac{E_f b t d^2}{2} \quad (\text{A.11})$$

Substituting the expression from Equation (A.11) into Equation (A.10) and introducing the non-dimensional geometric parameters similarly we get

$$\bar{\tau} = \bar{V} \left[\frac{\bar{c}}{\bar{c} + \bar{t}} + \frac{\bar{E}}{4} \frac{\bar{c}^3}{\bar{t}(\bar{c} + \bar{t})^2} \right] \quad (\text{A.12})$$

A.3 Global Buckling

The global buckling of the top facesheet of a sandwich beam can be predicted for $n = 1$ using the following expression

$$P_b = \frac{\pi^2 E_f b t^3}{12L^2} + \frac{E_c L^2}{\pi^2} \quad (\text{A.13})$$

The facesheet is assumed to be a simply supported beam resting on an elastic foundation. The buckling load P_b is non-dimensionalised by the Euler buckling load $P_{Eu_{ss}}$ of a simply supported facesheet with no elastic foundation.

$$P_{Eu_{ss}} = \frac{\pi^2 E_f b t^3}{12L^2} \quad (\text{A.14})$$

Dividing Equation (A.13) with Equation (A.14) and introducing the non-dimensional geometric parameters we get

$$\bar{P}_b = \frac{P_b}{P_{Eu_{ss}}} = 1 + \frac{12\bar{E}\bar{L}^4}{\pi^4\bar{b}\bar{t}^3} \quad (\text{A.15})$$

A.4 Local Buckling (Wrinkling)

The local buckling load P_w is non-dimensionalised by the Euler buckling load $P_{Eu_{cc}}$ of a clamped-clamped facesheet with no elastic foundation. Expression for Euler buckling load of a clamped-clamped facesheet with no elastic foundation can be written

as

$$P_{Eu_{cc}} = \frac{4\pi^2 E_f b t^3}{12L^2} \quad (\text{A.16})$$

Expression for predicting wrinkling of a facesheet

$$P_w = \frac{42E_f b t^3}{12L_w^2} + \frac{E_c L_w^2}{12} \quad (\text{A.17})$$

Dividing Equation (A.17) with (A.16)

$$\bar{P}_w = \frac{P_w}{P_{Eu_{cc}}} = 0.6161 \sqrt{\frac{\bar{E} \bar{L}^4}{\bar{b} \bar{t}^3}} \quad (\text{A.18})$$